FACULTY OF CHEMISTRY

DEPARTMENT OF PHYSICAL CHEMISTRY AND TECHNOLOGY OF POLYMERS

# Conducting polymer coatings exhibiting bacteria-responsive antibacterial properties-synthesis, structure, and mutual interactions

# Powłoki z polimerów przewodzących wykazujące właściwości antybakteryjne reagujące na obecność bakterii-synteza, struktura i wzajemne oddziaływania

**mgr. Abdullah**

**Supervisor: dr hab. inż. Katarzyna Krukiewicz, prof. PŚ**

**Gliwice 2026**

## Acknowledgements

I would like to express my sincere gratitude to the **National Science Centre (NCN), Poland**, for providing financial support for this doctoral research through the PRELUDIUM BIS project **No. 2021/43/O/ST5/02623**. This support made it possible to carry out the experimental work and complete the studies presented in this dissertation.

I am deeply grateful to my supervisor, **Prof. Katarzyna Krukiewicz**, for her continuous guidance, scientific advice, patience, encouragement, and trust throughout my Ph.D. studies. Her support played an essential role in shaping this research, strengthening my scientific thinking, and helping me develop as an independent researcher. I especially appreciate the time and effort she devoted to discussing my results, reviewing manuscripts, and guiding me through the different stages of my doctoral work.

I would also like to thank all members of the **Bioelectrochemistry Group at the Silesian University of Technology** for their support, cooperation, scientific discussions, and assistance during my doctoral studies. Working within the group provided a valuable research environment and many opportunities to exchange ideas, solve experimental problems, and develop the studies presented in this thesis.

My sincere thanks also go to all my collaborators, colleagues, and friends who supported me throughout this journey. I am grateful for their help in the laboratory, scientific discussions, encouragement, and friendship, which made the demanding periods of doctoral research much easier.

My deepest gratitude goes to my **family**, whose love, patience, understanding, and constant support have been a great source of strength throughout these years. Their encouragement helped me remain focused and motivated, especially during difficult moments and periods spent away from home.

Finally, I would like to thank everyone who, directly or indirectly, contributed to this work and supported me during my doctoral studies. This dissertation would not have been possible without their encouragement, assistance, and support.

## Table of contents

Abstract in English ..... 4
Abstract in Polish ..... 6
List of publications ..... 8
Nomenclature ..... 9
1. Introduction ..... 10
2. Hypothesis and research objectives ..... 13
3. Methodology ..... 15
3.1. Literature studies ..... 15
3.2. Electrode preparation and coating formation ..... 15
3.3. Surface functionalization strategies ..... 16
3.4. Bacterial growth and biofilm analysis ..... 17
3.5. Electrochemical and spectroelectrochemical characterization ..... 17
3.6. Physicochemical characterization ..... 18
3.7. Drug release and chromatographic analysis ..... 18
3.8. Antibacterial and cytocompatibility assays ..... 19
3.9. Statistical analysis ..... 19
4. Results and discussion ..... 20
4.1. Electroactive bacteria-conducting polymer biohybrids ..... 20
4.2. Organic-functionalized PEDOT:PSS interfaces ..... 26
4.3. Metal-ion-engineered PEDOT:PSS interfaces ..... 33
4.4. Surfactant-doped PEDOT antibacterial coatings ..... 40
4.5. Bacteria-responsive ceftazidime-loaded PEDOT coatings ..... 47
5. Summary ..... 63
6. Literature ..... 66
Summary of personal contribution ..... 74
List of Scientific Accomplishments ..... 77
Appendix: Supplementary information ..... 80

## Abstract

Conducting polymers have reversible redox activity, ionic transport, electrical conductivity, and the capacity to accommodate biologically active substances. These characteristics make them suitable for microbial electrochemical systems, but they also pose a challenging interface design problem. The electrode should facilitate bacterial adhesion, cell viability, and extracellular electron transfer in bioelectronic applications. On the other hand, in medical applications, the same tendency toward surface colonization must be suppressed before a mature biofilm is established. This dissertation examines both directions and develops a set of surface engineering strategies for controlling the interaction between PEDOT-based coatings and bacterial cells.

The first part of the work established the scientific basis for electrically conducting biohybrids by reviewing immobilization strategies, bacterial electron-transfer pathways, and the role of conducting polymers in linking biological and electronic charge transport. Two subsequent studies focused on improving the performance of PEDOT:PSS as a microbial electrode. Functionalization with organic compounds identified glucose as a particularly effective modifier, increasing *Shewanella oneidensis* MR-1 biofilm formation and cell viability while improving charge transfer between bacteria and the electrode. Modification with biologically relevant metal salts showed that calcium produced a favourable combination of roughness, wettability, cell viability, biofilm formation, and charge storage, whereas barium shifted the same material toward an antibacterial response.

The antibacterial part of the thesis investigated poly(3,4-ethylenedioxythiophene) (PEDOT) electropolymerized in the presence of dodecyltrimethylammonium bromide (DTAB). DTAB acted as a surfactant, dopant, structure-directing agent, and antibacterial component. The resulting PEDOT@DTAB coating stored substantially more charge than pristine PEDOT and inhibited biofilm formation by both *S. oneidensis* and *Pseudomonas aeruginosa*. Electrical stimulation accelerated DTAB release, demonstrating that the redox activity of the polymer could be used to regulate antibacterial release from the coating.

The major contribution of the dissertation was the development of a ceftazidime (CAZ)-loaded PEDOT coating that linked antibiotic release to bacterial redox activity.

Ceftazidime was incorporated during electropolymerization without compromising the charge-storage capability of PEDOT. Passive leakage remained low, whereas external electrical stimulation and interaction with electroactive bacteria produced substantially higher release. *S. oneidensis* and *P. aeruginosa* produced distinct electrochemical and spectroscopic responses, consistent with their different extracellular electron-transfer mechanisms. The coating reduced bacterial viability at the material interface, retained antibiofilm activity during prolonged incubation, and remained compatible with human dermal fibroblasts.

Taken together, the studies showed that PEDOT-based coatings could be designed either to support electroactive biofilms or to respond to bacterial colonization with localized antibacterial activity. The results provided a coherent foundation for future infection-responsive coatings for catheters, implants, wound dressings, and related bioelectronic devices.

## Streszczenie

Polimery przewodzące charakteryzują się odwracalną aktywnością redoks, zdolnością do transportu jonów, przewodnictwem elektrycznym oraz możliwością wbudowywania substancji biologicznie czynnych. Właściwości te sprawiają, że są one odpowiednimi materiałami do zastosowania w mikrobiologicznych układach elektrochemicznych, jednak jednocześnie stwarzają istotne wyzwania związane z projektowaniem interfejsu materiał–bakteria. W zastosowaniach bioelektronicznych powierzchnia elektrody powinna sprzyjać adhezji bakterii, utrzymaniu żywotności komórek oraz pozakomórkowemu transferowi elektronów. Z kolei w zastosowaniach medycznych ta sama tendencja do kolonizacji powierzchni powinna zostać ograniczona, zanim dojdzie do utworzenia dojrzałego biofilmu. W niniejszej rozprawie doktorskiej przeanalizowano oba te kierunki oraz opracowano strategie inżynierii powierzchni umożliwiające kontrolowanie oddziaływań pomiędzy powłokami na bazie PEDOT a komórkami bakteryjnymi.

W pierwszej części pracy określono podstawy naukowe dotyczące elektroprzewodzących materiałów biohybrydowych poprzez analizę strategii immobilizacji, bakteryjnych szlaków transferu elektronów oraz roli polimerów przewodzących w łączeniu biologicznego i elektronowego transportu ładunku. Dwa kolejne badania skupiły się na poprawie właściwości PEDOT:PSS jako materiału elektrodowego dla układów mikrobiologicznych. Funkcjonalizacja z wykorzystaniem związków organicznych wykazała, że glukoza była szczególnie skutecznym modyfikatorem, sprzyjającym tworzeniu biofilmu przez *Shewanella oneidensis* MR-1 oraz zwiększającym żywotność komórek, a jednocześnie usprawniającym transfer ładunku pomiędzy bakteriami a elektrodą. Modyfikacja z zastosowaniem soli metali wykazała natomiast, że wapń zapewniał korzystne połączenie chropowatości powierzchni, zwilżalności, żywotności komórek, tworzenia biofilmu oraz zdolności do magazynowania ładunku, podczas gdy bar nadawał temu samemu materiałowi właściwości ukierunkowane bardziej na działanie antybakteryjne.

W części rozprawy dotyczącej właściwości antybakteryjnych analizowano poli(3,4-etylenodioksytiofen) (PEDOT) otrzymywany metodą elektropolimeryzacji w obecności bromku dodecylotrimetyloamoniowego (DTAB). DTAB pełnił jednocześnie funkcję środka powierzchniowo czynnego, domieszki, czynnika kierującego strukturą

oraz składnika antybakteryjnego. Otrzymana powłoka PEDOT@DTAB wykazywała znacznie większą zdolność do magazynowania ładunku niż niemodyfikowany PEDOT oraz hamowała tworzenie biofilmu zarówno przez *S. oneidensis*, jak i *Pseudomonas aeruginosa*. Stymulacja elektryczna przyspieszała uwalnianie DTAB, wykazując tym samym, że aktywność redoks polimeru może być wykorzystana do regulowania uwalniania substancji antybakteryjnej z powłoki.

Najważniejszym osiągnięciem rozprawy było opracowanie powłoki PEDOT zawierającej ceftazydym (CAZ), w której uwalnianie antybiotyku było powiązane z aktywnością redoks bakterii. Ceftazydym został wprowadzony do matrycy polimerowej podczas elektropolimeryzacji bez pogorszenia zdolności PEDOT do magazynowania ładunku. Pasywne uwalnianie antybiotyku pozostawało na niskim poziomie, natomiast zewnętrzna stymulacja elektryczna oraz oddziaływanie z bakteriami elektroaktywnymi prowadziły do znacznie większego uwalniania CAZ. *S. oneidensis* oraz *P. aeruginosa* wywoływały odmienne odpowiedzi elektrochemiczne i spektroskopowe, co było zgodne z różnicami w mechanizmach pozakomórkowego transferu elektronów charakterystycznych dla tych gatunków. Powłoka zmniejszała żywotność bakterii na granicy faz materiał–bakteria, zachowywała właściwości antybiofilmowe podczas przedłużonej inkubacji oraz pozostawała kompatybilna z ludzkimi fibroblastami skóry.

Łącznie przeprowadzone badania wykazały, że powłoki na bazie PEDOT mogą być projektowane zarówno w celu wspierania rozwoju elektroaktywnych biofilmów, jak i w taki sposób, aby reagowały na kolonizację bakteryjną poprzez miejscowe działanie antybakteryjne. Uzyskane wyniki stanowią spójną podstawę do dalszego rozwoju powłok reagujących na obecność infekcji, przeznaczonych do zastosowania na cewnikach, implantach, opatrunkach oraz w innych urządzeniach bioelektronicznych.

## List of publications

The doctoral thesis presented is based on the following publications:

**[R1]** Abdullah; Krukiewicz, K. Development of electrically-conducting biohybrid materials based on electroactive bacteria and conjugated polymers: Review and perspectives. Electrochimica Acta 468 (2023) 143191. https://doi.org/10.1016/j.electacta.2023.143191.

JIF: 5.8; MNiSW: 100 points; Scopus Top 10

**[R2]** Abdullah; Shakibania, S.; Patel, T.; Shyntum, D. Y.; Krukiewicz, K. Surface-functionalized PEDOT:PSS interfaces for improved adhesion, viability, and extracellular charge transfer of Shewanella oneidensis MR-1. ACS Sustainable Chemistry & Engineering 12 (2024) 18508-18521. https://doi.org/10.1021/acssuschemeng.4c05458.

JIF: 7.6; MNiSW: 140 points; Scopus Top 10

**[R3]** Abdullah; Shyntum, D. Y.; Shakibania, S.; Patel, T.; Krukiewicz, K. Engineering conducting polymer-based interfaces for high-performance microbial electrochemical systems. Bioelectrochemistry 168 (2026) 109142. https://doi.org/10.1016/j.bioelechem.2025.109142.

JIF: 4.9; MNiSW: 100 points; Scopus Top 10

**[R4]** Abdullah; Shakibania, S.; Zabłocka-Godlewska, E.; Aniołek, K.; Krukiewicz, K. Surfactant-doped PEDOT films as dual-function bioelectronic coatings with enhanced charge storage capacity and antibiofilm activity. Bioelectrochemistry 172 (2026) 109366. https://doi.org/10.1016/j.bioelechem.2026.109366.

JIF: 4.9; MNiSW: 100 points; Scopus Top 10

**[R5]** Abdullah; Smołka, S.; Ayaz, K.; Shakibania, S.; Maryam, S.; Patel, T.; Turczyn, R.; Zabłocka-Godlewska, E.; Krukiewicz, K. Smart Antibacterial Coatings: Harnessing Bacterial Redox Activity for Infection Control. Advanced Materials Interfaces (2026) e70647. https://doi.org/10.1002/admi.70647.

JIF: 4.5; MNiSW: 100 points.

## Nomenclature

| | |
|---|---|
| **BES** | Bioelectrochemical system |
| **CA** | Chronoamperometry |
| **CAZ** | Ceftazidime |
| **CFU** | Colony forming unit |
| **CLSM** | Confocal laser scanning microscopy |
| **CP** | Conducting/conjugated polymer |
| **CPE** | Constant phase element |
| **CSC** | Charge storage capacity |
| **CV** | Cyclic voltammetry |
| **DLVO** | Derjaguin–Landau–Verwey–Overbeek theory |
| **DMEM** | Dulbecco's Modified Eagle Medium |
| **DTAB** | Dodecyltrimethylammonium bromide |
| **EDS** | Energy-dispersive X-ray spectroscopy |
| **EDOT** | 3,4-ethylenedioxythiophene |
| **EET** | Extracellular electron transfer |
| **EIS** | Electrochemical impedance spectroscopy |
| **EPS** | Extracellular polymeric substances |
| **FTIR** | Fourier-transform infrared spectroscopy |
| **HPLC** | High performance liquid chromatography |
| **ITO/PET** | Indium tin oxide on poly(ethylene terephthalate) |
| **LB** | Lysogeny broth |
| **MFC** | Microbial fuel cell |
| **MIC** | Minimum inhibitory concentration |
| **NHDF** | Normal human dermal fibroblasts |
| **OCP** | Open-circuit potential |
| **$OD_{600}$** | Optical density measured at 600 nm |
| **PBS** | Phosphate-buffered saline |
| **PDA** | Photodiode array detector |
| **PEDOT** | Poly(3,4-ethylenedioxythiophene) |
| **PEDOT:PSS** | Poly(3,4-ethylenedioxythiophene):poly(styrene sulfonate) |
| **PPy** | Polypyrrole |
| **Rct** | Charge transfer resistance |
| **Rs** | Solution resistance |
| **Sa** | Arithmetic mean surface roughness |
| **SEM** | Scanning electron microscopy |
| **WCA** | Water contact angle |

# 1. Introduction

Conducting polymers are organic macromolecules with conjugated backbones that permit charge delocalization along the polymer chain. Unlike conventional metallic conductors, most of them can exchange both electronic and ionic charge and can be reversibly oxidized and reduced in aqueous electrolytes. Poly(3,4-ethylenedioxythiophene) (PEDOT) and poly(3,4-ethylenedioxythiophene):poly(styrene sulfonate) (PEDOT:PSS) are of particular importance in bioelectronics because they combine high conductivity, high volumetric capacitance, chemical stability, and processability on flexible substrates. These features have led to their application in sensors, neural electrodes, organic electrochemical transistors, supercapacitors, and microbial electrochemical systems.[1,2]

In microbial electrochemical systems, conducting polymers are used as electrode coatings or as components of composite biointerfaces because their mixed electronic and ionic transport can support charge exchange between microbial redox pathways and the current collector. PEDOT, PEDOT:PSS, and polypyrrole (PPy) provide electroactive and chemically tunable surfaces for bacterial attachment while also participating in reversible redox and ion-exchange processes. Their usefulness therefore depends not only on intrinsic conductivity but also on how the polymer interface interacts with electroactive cells, redox proteins, and soluble mediators.[3,4]

Electroactive microorganisms such as *Shewanella oneidensis* (*S. oneidensis*) and *Pseudomonas aeruginosa* (*P. aeruginosa*) can exchange electrons with electrodes through direct contact, outer-membrane cytochromes, conductive pili, or diffusible redox shuttles. This process, referred to as extracellular electron transfer (EET), depends on the distance between cells and the electrode, biofilm formation, surface charge, and the availability of ions within the coating.[3,4]

Bacterial adhesion is therefore a decisive factor in the design of microbial electrodes. A highly conductive but biologically incompatible surface may support little biofilm and yield poor current generation. Conversely, a surface that supports a thick biofilm may still perform poorly when the cells are electrically isolated from the electrode. Surface roughness, wettability, charge, porosity, and chemical functionality all affect the first stage of attachment and the subsequent maturation of the biofilm. These parameters

are interdependent. For example, increasing roughness may provide protected anchoring sites, but the benefit can be lost when the surface charge strongly repels the charge on bacterial cells or when the coating blocks electron transfer.[5,6]

The same interfacial phenomena that are desirable in a microbial fuel cell (MFC) become a serious limitation in medical and bioelectronic devices. Bacterial colonization can progress from initial attachment to a mature biofilm embedded in an extracellular polymeric matrix. Once established, this hydrated matrix protects the cells, limits penetration of antimicrobial agents, and supports persistent communities that are difficult to eradicate. Device-associated biofilms can therefore reduce material performance and contribute to chronic infection, prolonged antimicrobial treatment, and, in severe cases, removal or replacement of the affected device.[7,8]

Consequently, conducting polymer coatings should be designed according to their intended biological role. For instance, a microbial anode requires stable adhesion, high viability, and efficient extracellular electron transfer. However, resistance to bacterial colonization, preservation of charge storage, and electrochemical communication with the electrode may alternatively be required for a wearable and implantable bioelectronic coating.[7,8]

In general, this dissertation examined both perspectives on the electrode-design problem. The first part provided a framework for understanding electrically conducting biohybrids formed from conjugated polymers and electroactive microorganisms [**R1**]. The second part used organic substances, particularly carbohydrates, polymers, and adhesion promoters, to modify the PEDOT:PSS interface and improve *S. oneidensis* adhesion, viability, and extracellular electron transfer [**R2**]. The third part used biologically relevant metal ions to modify polymer structure, surface charge, and bacterial physiology [**R3**]. The fourth part incorporated dodecyltrimethylammonium bromide (DTAB) during 3,4-ethylenedioxythiophene (EDOT) electropolymerization to develop a dual-function coating that combined high charge storage with electrically controlled antibiofilm activity [**R4**]. In the fifth part, the antibiotic ceftazidime (CAZ) was incorporated into the PEDOT matrix and released in response to bacterial redox activity [**R5**].[3,9]

Although these five parts address different applications, they are united by a common scientific question: how can the molecular and physicochemical properties of a

conducting polymer interface be tailored to control interactions between the polymer and bacterial cells? Addressing this question required consideration of factors beyond conductivity alone. Surface roughness, wettability, charge storage capacity, polymer redox state, bacterial metabolism, extracellular electron transfer, and the mobility of incorporated ions or therapeutic agents all contributed to the overall interfacial response. The final PEDOT@CAZ study integrated these elements by considering bacterial electron transfer not only as a measurable bioelectrochemical phenomenon, but also as a mechanism capable of triggering localized drug release.[10,11]

## 2. Hypothesis and research objectives

I hypothesized that bacterial and conducting polymer interactions can be programmed through the interfacial properties of PEDOT-based coatings, such that the same electroactive platform can be tailored either to promote extracellular electron transfer or to convert bacterial electrical activity into a localized antibacterial response. I further hypothesized that this functional switching can be achieved by independently tuning surface roughness, wettability, interfacial charge, polymer redox state, dopant chemistry, and ion exchange, thereby establishing defined structure, interface, and function relationships.

Based on these hypothesis, the following research objectives were formulated and achieved:

**1.** To conduct a comprehensive literature review on the immobilization of whole bacterial cells and bacterial redox proteins on conjugated polymers, with particular emphasis on PEDOT, PEDOT:PSS, and polypyrrole, as well as the mechanisms governing extracellular electron transfer.

**2**. To identify the key surface and biological parameters that govern bacterial adhesion, viability, biofilm formation, and extracellular charge transfer at conducting polymer interfaces.

**3**. To prepare PEDOT:PSS coatings functionalized with selected carbohydrates, polysaccharides, and adhesion-promoting macromolecules, and to evaluate their effects on the adhesion, viability, biofilm formation, and extracellular electron transfer of *S. oneidensis* MR-1.

**4**. To investigate whether biologically relevant metal salts can modify PEDOT:PSS through ionic coordination or crosslinking, thereby enhancing bacterial attachment and electrochemical performance.

**5**. To compare the species-dependent effects of calcium, iron, magnesium, manganese, and barium modifications on biofilm formation, bacterial viability, charge-storage capacity, and charge transfer resistance.

**6**. To electropolymerize EDOT in the presence of DTAB and evaluate whether the surfactant can simultaneously function as a dopant, structure-directing agent, and antibacterial component.

**7**. To quantify passive and electrically triggered DTAB release and to relate the release behaviour to antibiofilm activity against *S. oneidensis* and *P. aeruginosa*.

**8**. To incorporate ceftazidime into PEDOT during electropolymerization and determine how drug loading influences the polymer's redox behaviour, charge storage capacity, charge transfer resistance, surface morphology, and wettability.

**9**. To compare passive, electrically induced, and bacteria-triggered ceftazidime release, and to distinguish electroactivity-driven release from nonspecific effects associated with bacterial growth or pH variation.

**10**. To characterize species dependent redox interactions between PEDOT-based coatings and *S. oneidensis* or *P. aeruginosa* using cyclic voltammetry, electrochemical impedance spectroscopy, spectroelectrochemistry, open-circuit potential measurements, chronoamperometry, and chronopotentiometry.

**11**. To determine whether PEDOT@CAZ can inhibit bacterial adhesion, reduce biofilm formation, retain antibacterial activity during prolonged exposure, and remain cytocompatible toward mammalian fibroblasts.

# 3. Methodology

The experimental and analytical procedures used in the five research parts are compiled in this chapter. Instead of being explained individually for every study, the methods are arranged based on their functional purpose to avoid duplication.

## *3.1. Literature studies*

The literature review focused on conducting and conjugated polymers, electroactive bacteria, microbial fuel cells, bacterial immobilization, antibacterial properties, surface adhesion, and the mechanisms of extracellular electron transfer. The literature was obtained through multiple databases such as Elsevier (https://www.elsevier.com/en), Science Direct (http://www.sciencedirect.com), PubMed (http://www.ncbi.nlm.nih.gov/pubmed), Google Scholar (http://www.scholar.google.com) , Wiley (http://www.onlinelibrary.wiley.com), Springer (http://www.springer.com), and Scopus (http://www.scopus.com). Searches combined terms such as PEDOT, PEDOT:PSS, polypyrrole, electroactive bacteria, exoelectrogen, electrotroph, biofilm, antibacterial, drug delivery, bacterial immobilization, c-type cytochrome, flavin, pyocyanin, microbial fuel cell, biosensor, and biohybrid material. Peer-reviewed articles describing whole-cell immobilization, bacterial protein immobilization, conducting polymer electrodes, and electrochemical analysis of bacterial biofilms were critically evaluated. Particular attention was paid to studies that connected immobilization strategy with measurable changes in current, impedance, charge storage, or power output [**R1**].[2,3]

## *3.2. Electrode preparation and coating formation*

For the PEDOT:PSS studies, commercial indium tin oxide-coated poly(ethylene terephthalate) (ITO/PET) foils were used as flexible conducting substrates for electrochemical measurements, while glass slides were used for selected microbiological experiments. An aqueous PEDOT:PSS dispersion was deposited by drop-casting and dried at 50 °C. Organic modifiers (glucose, sucrose, maltose, cellulose, chitosan, poly(vinyl alcohol), poly-L-lysine, and laminin) or metal salt solutions ($FeCl_3$, $MgSO_4$, $MnCl_2$, $CaCl_2$, and $BaCl_2$) were subsequently deposited on the polymer surface and dried at a lower temperature to maintain film integrity and allow interfacial reorganization [**R2**, **R3**].[12,13]

For the DTAB and CAZ studies, PEDOT was formed electrochemically from a 10 mM EDOT dispersion in phosphate-buffered saline (PBS; 0.01 M phosphate buffer, 0.0027 M potassium chloride, and 0.137 M sodium chloride). Electropolymerization was performed in a three-electrode cell using ITO/PET as the working electrode, Ag/AgCl as the reference electrode, and a Pt/Ti rod as the counter electrode. Twenty cyclic-voltammetry scans were applied between -0.8 V and +1.5 V vs. Ag/AgCl at 0.1 V $s^{-1}$. DTAB or CAZ was introduced into the monomer dispersion at 1 mM, corresponding to an EDOT:additive molar ratio of 10:1. The resulting PEDOT@DTAB and PEDOT@CAZ films were rinsed thoroughly to remove residual monomer and loosely associated additive before characterization [**R4**, **R5**].[9,14]

### *3.3. Surface functionalization strategies*

Organic functionalization was performed using glucose, sucrose, maltose, cellulose, chitosan, poly(vinyl alcohol), poly-L-lysine, and laminin. These modifiers were selected to represent nutritional carbohydrates, roughness-increasing polysaccharides, film-forming polymers, and established adhesion promoters. The solutions were drop-casted onto PEDOT:PSS and dried at 35 °C. The resulting coatings were designated PEDOT:PSS@Glucose, PEDOT:PSS@Sucrose, PEDOT:PSS@Maltose, PEDOT:PSS@Cellulose, PEDOT:PSS@Chitosan, PEDOT:PSS@PVA, PEDOT:PSS@PLL, and PEDOT:PSS@Laminin [**R2**].[6,12]

Metal ion functionalization was carried out by drop-casting using 1 mM aqueous solutions of $FeCl_3$, $MgSO_4$, $MnCl_2$, $CaCl_2$, and $BaCl_2$. Slow drying at 35 °C for one hour was used to promote partial penetration of multivalent ions into PSS-rich regions. The working interpretation was that the cations could coordinate with sulfonate groups, screen negative charge, alter PEDOT/PSS phase organization, and create ion-dependent surface structures. Ion retention after immersion in PBS was evaluated by EDS [**R3**].[13,15]

Drug loading was performed in situ rather than by post-deposition soaking. Ceftazidime was present during EDOT electropolymerization, allowing it to become physically entrapped and non-covalently associated with the growing PEDOT matrix. This method was selected to preserve the pharmacological structure of the antibiotic while encapsulating it inside a redox-active material capable of ion exchange [**R5**].[9,16]

### *3.4. Bacterial growth and biofilm analysis*

*S. oneidensis* MR-1 (LMG 19005) and *P. aeruginosa* (LMG 1242) were obtained from the Belgian Coordinated Collections of Microorganisms. Lyophilized cultures were revived in lysogeny broth (LB) and incubated at 37 °C with shaking. Single colonies were used to prepare overnight cultures, which were diluted into fresh medium and grown to the exponential phase. Cell density was standardized to approximately 0.5 McFarland, corresponding to about $1 \times 10^8$ colony-forming units (CFU) $mL^{-1}$ [**R2-R4**].[9,14]

Biofilm formation was quantified by crystal violet staining. After incubation, loosely attached cells were removed by gentle washing, the remaining biofilm was fixed with methanol, stained with 1% crystal violet, and destained with 33% acetic acid. Absorbance at 570 nm was used to calculate biofilm formation or biofilm inhibition relative to the selected control. Cell viability was evaluated with the LIVE/DEAD BacLight kit. SYTO 9-labelled cells were visualized as viable, whereas propidium iodide-labelled cells were considered membrane-compromised or dead. Confocal fluorescence microscopy and ImageJ analysis were used to determine the relative proportions of live and dead bacteria [**R2-R4**].[17,18]

In the long-term PEDOT@CAZ experiments, biofilm formation was monitored for eight days, and bacterial morphology was evaluated by SEM after chemical fixation, graded ethanol dehydration, and gold sputter coating. These measurements were used to distinguish a simple reduction in biomass from stress related changes in cell dimensions and extracellular matrix formation [**R5**].[9,18]

### *3.5. Electrochemical and spectroelectrochemical characterization*

Cyclic voltammetry (CV) was used to monitor polymer formation, identify redox features, calculate charge storage, and assess bacterial electroactivity. Electrochemical impedance spectroscopy (EIS) was used to distinguish solution resistance, interfacial charge-transfer resistance, and non-ideal capacitive behaviour. For bacterial biofilms, the potential window and scan rate were reduced to avoid electrochemical stress while preserving the redox signals associated with extracellular electron transfer. These methods were complemented by open-circuit potential (OCP) monitoring, chronoamperometry at +0.1 V, and chronopotentiometry at 10 μA to follow short-time electron-transfer dynamics [**R5**].[19,20]

Charge storage capacity (CSC) was calculated from the integrated area of the cyclic voltammogram according to:

$$CSC = \frac{1}{S\nu}\int_{E_1}^{E_2} I(E)dE$$

where S is the geometrical electrode area ($cm^2$), ν is the scan rate ($V\ s^{-1}$), $E_1$ and $E_2$ are the lower and upper cutoff potentials (V), respectively, and I(E) is the measured current (A).

A larger CSC indicates a greater capacity for reversible charge exchange within the selected potential range; however, it does not necessarily correspond to lower charge transfer resistance or more efficient charge transfer across the bacteria–electrode interface. Spectroelectrochemical measurements were used to connect the optical response of PEDOT with its oxidation state. The potential was stepped between +0.5 V and -0.5 V vs. Ag/AgCl, and UV-Vis spectra were collected from 200 to 800 nm after each step. Sterilized PEDOT films were then incubated with *S. oneidensis* or *P. aeruginosa* for 24 h and measured without an external stimulus. This comparison provided an independent indication of whether bacterial activity shifted PEDOT toward a more reduced, oxidized, or mixed redox state [**R5**].[21,22]

### *3.6. Physicochemical characterization*

Fourier-transform infrared spectroscopy (FTIR) was used to confirm the chemical signatures of PEDOT:PSS, organic modifiers, metal-ion interactions, DTAB, and CAZ incorporation. Scanning electron microscopy (SEM) provided information on film morphology and bacterial attachment. Energy-dispersive X-ray spectroscopy (EDS) was used to identify the elemental composition of the coatings and to confirm the presence of modifier-specific elements, including nitrogen from CAZ. Surface roughness was calculated from SEM images, while static water contact angle (WCA) measurements were used to compare wettability. Together, these measurements allowed chemical incorporation to be related to the interfacial properties experienced by bacterial cells [**R2-R5**].[6,23]

### *3.7. Drug release and chromatographic analysis*

Passive release experiments were carried out by immersing PEDOT@DTAB or PEDOT@CAZ films in PBS without electrical stimulation. Electrically triggered release was generated by repeated CV scans. DTAB concentration was quantified by ultraviolet

visible (UV-Vis) spectroscopy, whereas ceftazidime concentration was quantified by high performance liquid chromatography (HPLC) using a C18 column and photodiode array detection at 258 nm. Separate calibration curves were prepared in PBS and LB to account for matrix effects. Bacteria-triggered CAZ release was measured after 24 h exposure to *S. oneidensis*, *P. aeruginosa*, *Staphylococcus aureus* (*S. aureus*), or *Escherichia coli* (*E. coli*). Sterile media adjusted to acidic and alkaline pH values were used as additional controls [**R4**, **R5**].[24,25]

For PEDOT@CAZ, the minimum inhibitory concentration (MIC) of free ceftazidime was determined by agar well diffusion and broth microdilution assays. The amount released from the coating was then compared with the MIC values to determine whether the local dose was sufficient to explain the antibacterial response. The distinction between total measured release and biologically available drug was retained in the interpretation because ceftazidime can degrade in aqueous media and can be inactivated by bacterial beta lactamases [**R5**].[26,27]

### *3.8. Antibacterial and cytocompatibility assays*

Antibacterial performance was assessed through optical density, crystal violet biofilm quantification, confocal LIVE/DEAD imaging, and SEM. The purpose of using several assays was to separate growth in the bulk medium from the response at the coating interface. Cytocompatibility of ITO/PET, PEDOT, and PEDOT@CAZ was evaluated with normal human dermal fibroblasts (NHDFs). Cells were cultured directly on the films, and metabolic activity was measured after 48 h using the Alamar Blue assay with material and medium blanks [**R5**].[28,29]

### *3.9. Statistical analysis*

Experiments were performed in independent triplicates unless otherwise specified. Results are presented as mean values with standard deviations. Statistical significance was evaluated using one-way analysis of variance or two-group comparisons with a significance threshold of $p < 0.05$. Electrochemical data were processed in OriginPro and fitted with EIS Spectrum Analyzer, while microscopic images were analysed in ImageJ [**R2**-**R5**].[30]

# 4. Results and discussion

## *4.1. Electroactive bacteria-conducting polymer biohybrids*

### *4.1.1. Scientific background and scope of the review*

In the first publication, I reviewed the development of electrically conducting biohybrid materials formed by combining electroactive bacteria with conjugated polymers. The study was motivated by the observation that conducting polymers can act as more than passive electrode coatings. Their redox state, charge density, ion exchange, and surface properties can change in response to the surrounding biological environment. At the same time, electroactive microorganisms introduce metabolic electron transfer pathways, redox proteins, secreted mediators, and self-organized biofilms. When bacteria and conducting polymers are brought into close contact, the resulting interface can exhibit properties that are not present in either part alone [**R1**].[3,10] The most significant interfaces were PEDOT, PEDOT:PSS, and PPy, which provided reversible oxidation and reduction, pseudocapacitive charge storage, and mixed electronic/ionic transport. PEDOT:PSS is water-processable and mechanically compatible with flexible substrates, making it applicable in bioelectronics. PPy can be coated electrochemically or chemically around bacterial cells and retain cell viability under regulated polymerization conditions.[31]

The central conclusion of the review was that bacterial cell immobilization should be regarded as a functional design step rather than simply a means of retaining cells on the electrode surface. The performance of the resulting biohybrid system depends on the number of viable cells, their proximity to the electrode, the formation of the extracellular matrix, the accessibility of redox proteins, and the efficiency with which electrons or redox mediators can move through the polymer. A high cell density is therefore beneficial only when the immobilized cells remain effectively connected to the current collector.[3,32]

### *4.1.2. Immobilization strategies and interfacial requirements*

Three main bacterial cell immobilization strategies were compared: adsorption, antibody-mediated immobilization, and electrically induced immobilization as shown in **Figure 1.** Adsorption is experimentally straightforward and relies on natural cell adhesion, extracellular polymeric substances, hydrophobic interactions, and surface topography. Its main limitation is that attachment may be relatively weak and highly sensitive to factors

such as pH, ionic strength, nutrient availability, surface roughness, and wettability. Rough surfaces can provide cracks and protrusions that protect cells from shear forces.[3,5]

Antibody-mediated immobilization provided biological specificity and is particularly useful for pathogen detection. A selected antibody can bind to a target bacterium on a conducting-polymer based sensor, producing a measurable change in resistance or impedance. However, antibody-based interfaces are relatively expensive, may lose activity, and often result in lower cell coverage than nonspecific adsorption. This strategy is therefore well suited to sensing applications but is less appropriate for microbial fuel cells, where a dense and metabolically active biofilm is typically required.[3,33]

Electrically induced immobilization exploits the tunable redox state of a conducting polymer to attract charged bacterial components during electrodeposition or electropolymerization. Most bacterial surfaces carry a net negative charge, whereas oxidized PEDOT and PPy contain positively charged sites. This electrostatic interaction can facilitate the incorporation of bacterial cells into the growing polymer matrix. However, the process must be carefully controlled, as high current densities, large potential windows, or strongly oxidizing conditions can damage cell membranes and reduce bacterial viability.[3,32]

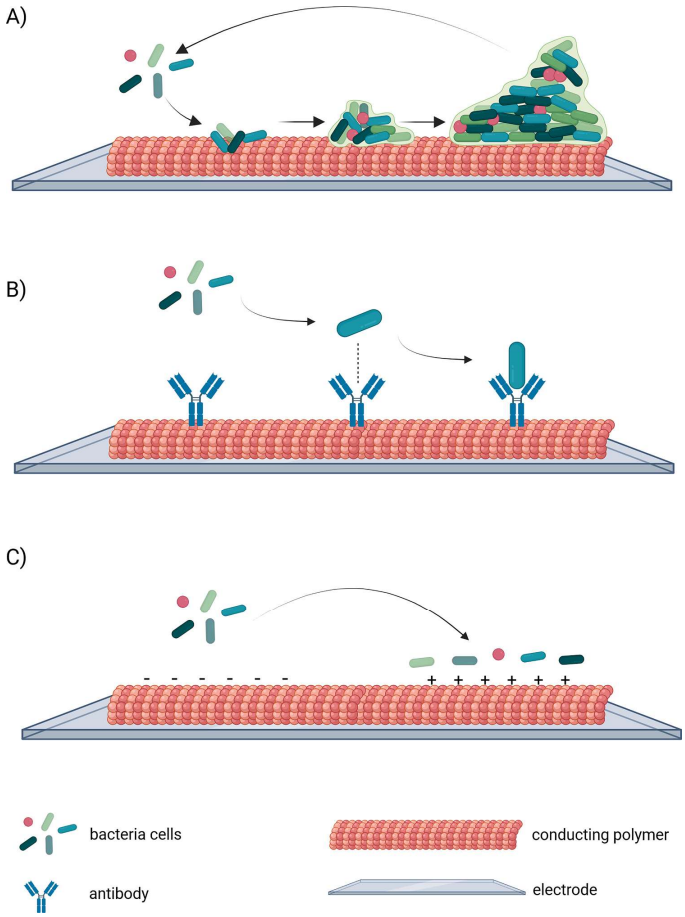



***Figure 1**: Principal routes for immobilizing bacterial cells on conducting-polymer surfaces: adsorption (A), antibody-mediated immobilization (B), and electrically induced immobilization (C). Reproduced from Figure 2 in [R1]. Copyright (2023) Electrochimica Acta published by Elsevier.*

### *4.1.3. Molecular mechanisms of adhesion and electron transfer*

Bacterial attachment to a conducting polymer is regulated by a chemically diverse cellular surface. Polysaccharides, proteins, lipids, nucleic acids, fimbriae, pili, and flagella play an important role in the initial attachment (**Figure 2A**). Upon attachment, extracellular polymeric substances form a hydrated matrix that facilitates cell growth and retains nutrients and electron shuttles. The electric double layer and short-range interactions described by Derjaguin-Landau-Verwey-Overbeek (DLVO) theory contribute to the initial approach, while bacterial appendages such as pili and fimbriae and extracellular polymer secretion become increasingly important as the biofilm develops.[6]

Electroactive bacteria contain specialized pathways for transferring electrons beyond the cytoplasmic membrane. In *S. oneidensis*, electrons move from the quinol pool through CymA and the MtrCAB complex to outer-membrane cytochromes (**Figure 2B**). These electrons may reach the electrode either directly or through secreted flavins that function as diffusible redox shuttles. *P. aeruginosa*, in contrast, produces phenazine compounds, such as pyocyanin, that facilitate mediated electron transfer. These pathways allow bacterial cells to modify the redox environment at the polymer interface even when not all cells are in direct physical contact with the electrode surface.[34,35]

The polymer responds dynamically to this biological electron flux. Changes in its oxidation state alter the density of charge carriers, polymer-chain conformation, ion uptake, and surface wettability. Consequently, bacterial activity can partially reduce or oxidize the conducting matrix, while the physicochemical properties of the matrix can, in turn, influence bacterial adhesion and local metabolism.[1,10]

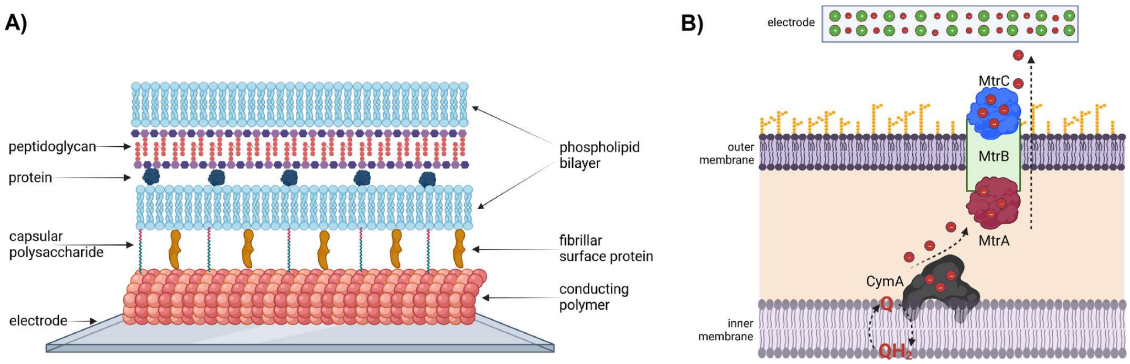



***Figure 2**: Schematic representation of bacterial outer-membrane structures involved in adhesion (A) and the Mtr pathway for extracellular electron transfer in S. oneidensis (B). Reproduced from Figure 9 in [R1]. Copyright (2023) Electrochimica Acta published by Elsevier.*

### *4.1.4. Electrochemical consequences and research gaps*

An effective biohybrid interface should reduce the resistance of biologically relevant charge-transfer pathways, increase current generation, improve power output, or support stable and reversible electron exchange. PEDOT:PSS-based bacterial composites have been reported to produce substantially higher steady-state currents than unmodified carbon electrodes. Previous comparative studies using wild-type and mutant *S. oneidensis* strains showed that both direct cytochrome-mediated contact and flavin-mediated electron

transfer contribute to the overall electrochemical response (**Figure 3A, B**).[3,36] Coating *S. oneidensis* cells with PPy provided a particularly clear demonstration of this effect. The conducting polymer matrix may form an electrical bridge between the outer-membrane cytochromes and the carbon-cloth current collector (**Figure 3C**). The PPy-coated bacterial anode achieved a maximum power density of 147.9 μW $cm^{-2}$, compared with 9.8 μW $cm^{-2}$ for the uncoated bacterial control (**Figure 3A, B**). This improvement was accompanied by lower charge-transfer resistance and a stronger electrochemical response, indicating that the PPy coating enhanced electrical conductivity throughout the bacterial layer rather than simply increasing the surface area.[32]

Apart from summarizing the current state of the art, in **R1** I also identified several important research gaps. The extent to which different bacterial species oxidize or reduce PEDOT and PPy remains insufficiently understood. Further investigation is needed to determine how immobilization influences gene expression, cellular metabolism, mediator production, and the organization of outer-membrane redox proteins. Long-term studies must also distinguish biological electron transfer from changes arising from polymer swelling, cell death, or the accumulation of electrically insulating biomass. These questions provided the rationale for the subsequent experimental studies presented in this thesis.[3,37]

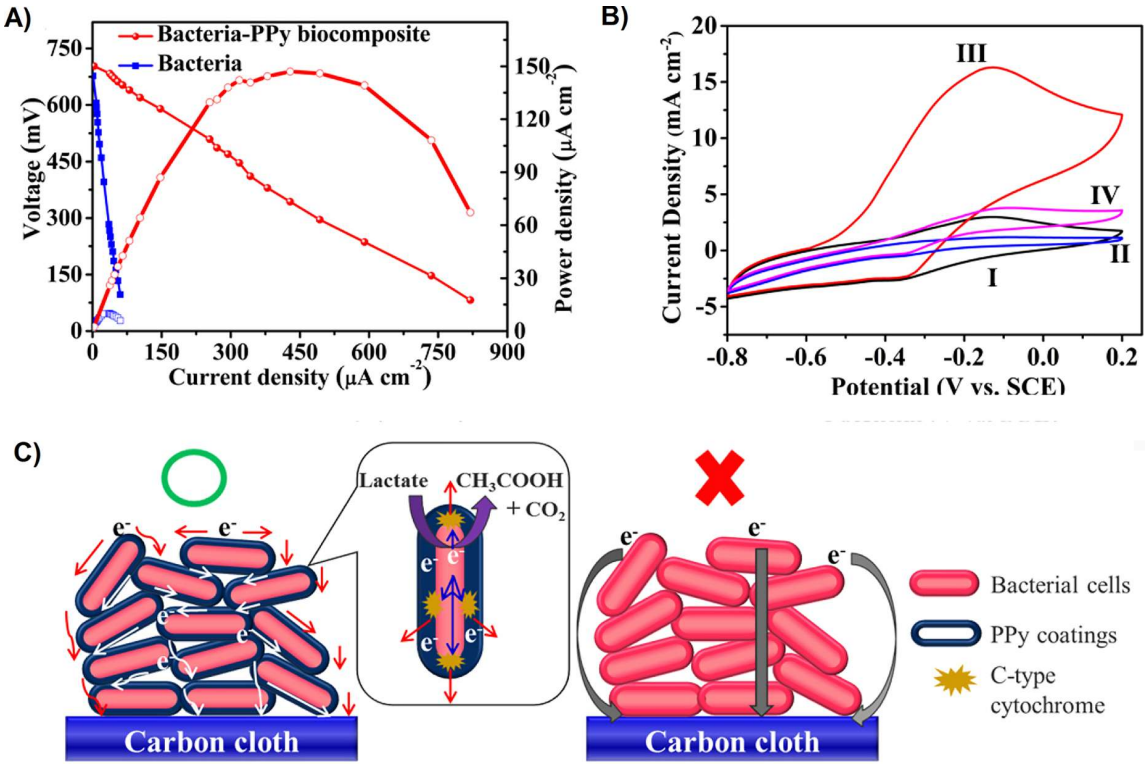



***Figure 3**: Electrochemical performance of PPy-coated S. oneidensis cells, including polarization and power-density behaviour (A), cyclic voltammetry (B), and the proposed conductive contact mechanism (C). Adapted from Song et al.[32] Copyright (2017) Angewandte Chemie International Edition Published by Wiley-VCH GmbH.*

**In this chapter, I determined that conducting-polymer/bacteria systems should be designed as integrated biointerfaces. This chapter brought together immobilization chemistry, bacterial physiology, polymer redox behaviour, and electrochemical performance within a single framework. It also showed that the same interfacial parameters can be exploited in different ways: they may be optimized to promote electroactive biofilm formation in microbial fuel cells or deliberately modified to inhibit bacterial colonization on biomedical coatings. This conceptual framework guided the selection of surface modifiers and analytical approaches used in the subsequent experimental studies.**[3,33]

## 4.2. Organic-functionalized PEDOT:PSS interfaces

### *4.2.1. Research problem and material design*

The second publication translated the design principles identified in the first chapter into a systematic experimental investigation. PEDOT:PSS is widely used in bioelectronics; however, its relatively smooth surface and the presence of negatively charged PSS-rich domains can limit bacterial adhesion. I therefore investigated whether a simple secondary coating could create a more favourable interface for *S. oneidensis* while preserving the electrochemical functionality of PEDOT:PSS [**R2**].[6,12]

The selected modifiers were chosen to represent distinct interfacial mechanisms and were drop-cast onto a PEDOT:PSS film (**Figure 4A**). Glucose, sucrose, and maltose were expected to create carbohydrate-rich surfaces and, in some cases, provide a metabolic benefit. Cellulose and chitosan were selected as polysaccharides capable of increasing surface roughness and modifying interfacial charges. PVA was included as a film-forming polymer, whereas poly-L-lysine and laminin were used as established adhesion-promoting macromolecules. The aim was not simply to identify the roughest or most hydrophilic surface, but rather to determine which combination of surface chemistry and morphology provided the most favourable biological and electrochemical interface.[6,12]

FTIR spectroscopy confirmed the presence of the selected modifiers through characteristic O–H, C–H, N–H, and amide-related absorption bands (**Figure 4B**, **C**, and **D**). EDS analysis further indicated that most secondary coatings provided extensive coverage of the PEDOT:PSS surface, as reflected by the marked reduction or absence of the sulfur signal originating from the underlying polymer. SEM imaging revealed clear differences in surface morphology: carbohydrate-based coatings produced relatively smooth surfaces, whereas cellulose, chitosan, and poly-L-lysine formed larger agglomerated structures. PVA generated a comparatively smoother and more continuous film, while laminin produced distinct discrete surface features.[12,38]

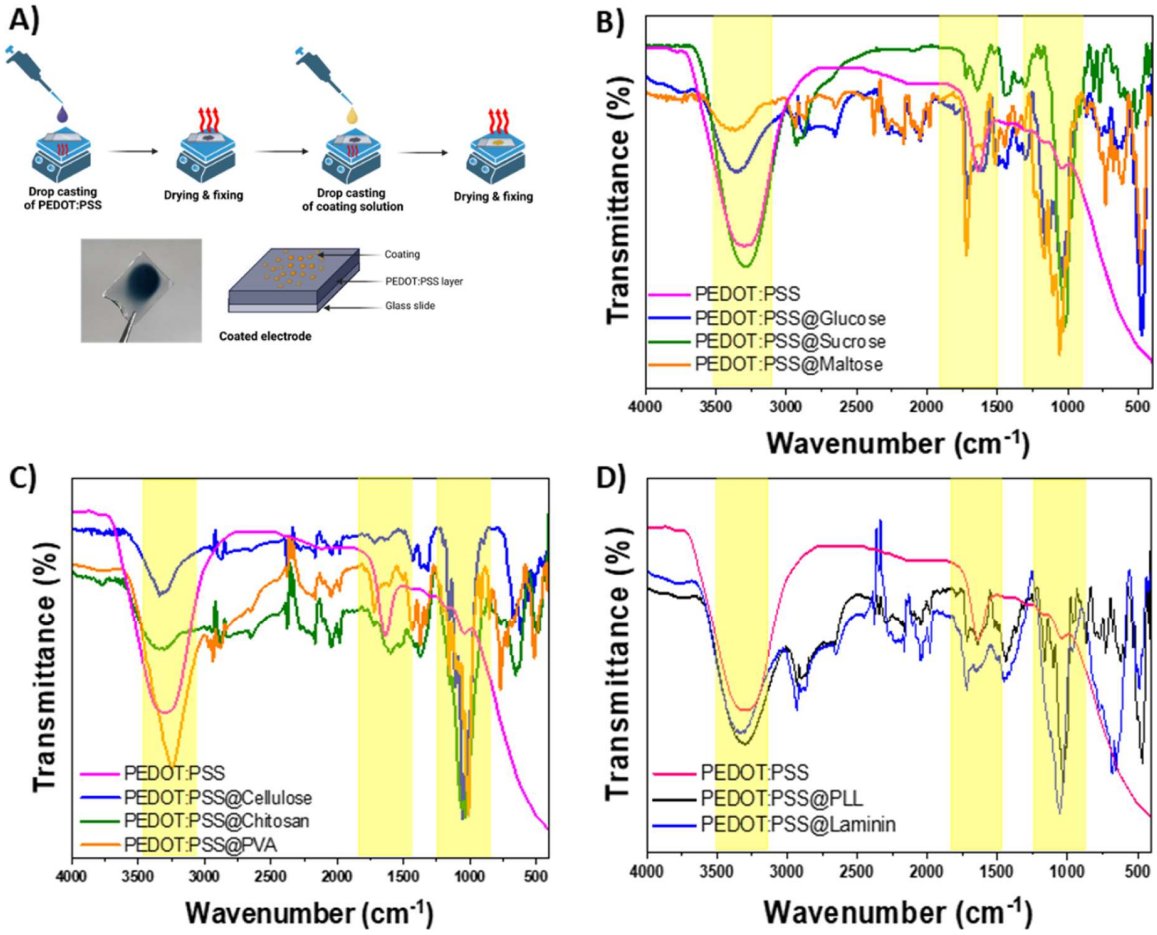



***Figure 4**: Preparation of organic-functionalized PEDOT:PSS films (A), and FTIR spectra confirming carbohydrate (B), polymer (C), and adhesion-promoter coatings (D). Reproduced from Figure 1 in [R2]. Copyright (2024) ACS Sustainable Chemistry & Engineering published by American Chemical Society.*

### *4.2.2. Surface roughness, wettability, and abiotic electrochemistry*

Pristine PEDOT:PSS exhibited a low average surface roughness of 0.10 ± 0.04 µm, providing relatively few anchoring sites for bacterial attachment. Surface functionalization substantially increased the surface roughness, thereby creating a more topographically complex interface for bacterial adhesion. The highest values were obtained for PEDOT:PSS@PLL (2.8 ± 0.5 µm), PEDOT:PSS@Chitosan (2.7 ± 0.8 µm), and PEDOT:PSS@Cellulose (2.6 ± 0.8 µm). PEDOT:PSS@Glucose and PEDOT:PSS@Laminin both reached approximately 2.1 ± 0.5 µm and 2.1 ± 0.6 µm, respectively, placing them within the range generally favourable for attachment.[6,12] All coatings were hydrophilic or moderately hydrophilic, with water contact angles below 90°.

Chitosan exhibited the highest contact angle, 82.9 ± 5.2°, whereas sucrose and PVA reduced the contact angle to approximately 17.1 ± 2.0° and 19.1 ± 3.9°, respectively. Glucose maintained an intermediate contact angle of around 69.2 ± 1.5°, providing a moderately hydrophilic surface. These findings demonstrate that the coatings could not be evaluated on the basis of a single surface parameter. For example, cellulose exhibited high roughness but supported limited biofilm formation (as shown in the next section), whereas glucose combined increased roughness, moderate wettability, and potential nutritional relevance.[5,12]

Furthermore, pristine PEDOT:PSS was able to store charge of 23.1 ± 2.7 mC $cm^{-2}$ and passed a maximum current density of 0.91 ± 0.01 mA $cm^{-2}$. The organic coatings reduced these values because they introduced electrically insulating material at the electrolyte interface. PEDOT:PSS@Glucose, for example, stored charge of 176.0 ± 10.3 μC $cm^{-2}$ and passed 15.0 ± 1.5 μA $cm^{-2}$. Similarly, EIS showed increased charge-transfer resistance. This initial loss of conductivity was important because it may explain that any improvement after bacterial colonization would have to arise from a better biological interface rather than from a more conductive abiotic film.[1,12]

### *4.2.3. Biofilm formation and bacterial viability*

The biological results identified glucose as the most effective modifier. Pristine PEDOT:PSS supported only 3.3 ± 1.3% biofilm formation and 42.1 ± 2.1% viable cells. PEDOT:PSS@Glucose increased biofilm formation to 54.8 ± 1.2% and bacterial viability to 97.5 ± 1.5% (**Figure 5A**, **B**, and **C**). Sucrose, chitosan, poly-L-lysine, and laminin also supported biofilm formation above 40%, whereas maltose, cellulose, and PVA produced only modest improvements.[12]

The glucose additive effect can be interpreted through both the surface chemistry of the coating and microbial physiology. The modified surface was rough enough to provide anchoring sites and remained moderately hydrophilic. In addition, glucose can participate in *S. oneidensis* metabolism and in the biosynthesis of surface-associated carbohydrates. Metabolic conversion of glucose contributes to extracellular matrix production and can increase riboflavin-associated signaling and biofilm development. The coating therefore did not function merely as a passive adhesive layer; rather, it created a

local microenvironment that promoted bacterial attachment, maintained cell viability, and supported extracellular matrix formation.[12,15]

The cellulose coating demonstrated why roughness alone is insufficient. Although PEDOT:PSS@Cellulose had one of the highest roughness values, it supported only a small fraction of biofilm. The likely explanation is that surface charge and the organization of the hydrated polymer layer remained unfavourable. This difference was one of the most useful findings of the study because it showed that topography must be interpreted together with chemistry and bacterial metabolism.[5,12]

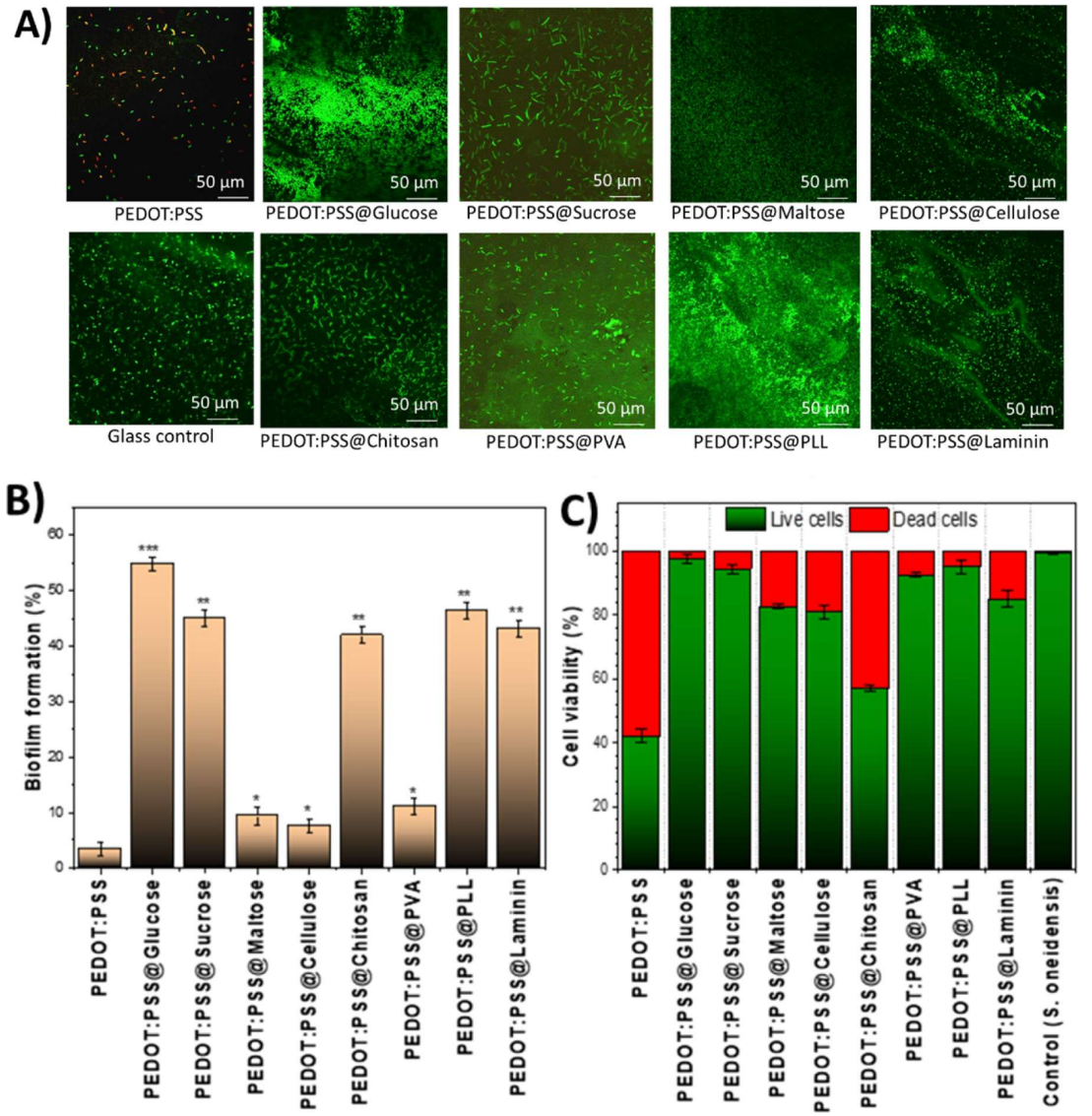



***Figure 5**: Confocal microscopy images (A), biofilm formation (B), and LIVE/DEAD viability of S. oneidensis on pristine and organically modified PEDOT:PSS films (C). Reproduced from Figure 6 in [R2]. Copyright (2024) ACS Sustainable Chemistry & Engineering published by American Chemical Society.*

### *4.2.4. Extracellular charge transfer and significance*

Electrochemical measurements after bacterial incubation were performed for pristine PEDOT:PSS and the glucose-functionalized PEDOT:PSS electrode, because glucose had produced the most favourable biological response. *S. oneidensis* increased the current response of PEDOT:PSS@Glucose despite its lower abiotic conductivity. The most important evidence came from impedance spectroscopy. In the absence of bacteria,

PEDOT:PSS@Glucose had a higher charge transfer resistance (Rct) than pristine PEDOT:PSS because of the insulating carbohydrate layer. After biofilm formation, however, Rct of the glucose-functionalized interface decreased markedly, whereas Rct of pristine PEDOT:PSS increased (**Figure 6A-C**).[12,36]

This reversal in activity shows that the glucose layer improved the bacteria electrode biointerface. In a dense, viable biofilm, outer-membrane cytochromes and flavins were near the polymer and the biochemical pathways then overcame the abiotic barrier to improve interfacial charge exchange (**Figure 6D**).[12,34] This study also offered practical advantages. The modification was achieved through a simple drop-casting procedure, required no complex coupling chemistry, and relied on a low-cost, biocompatible carbohydrate. The main limitations included the potential dissolution of the modifier, the use of nutrient-rich LB medium, and the relatively short 24 h incubation period. Future studies should investigate glucose retention in polymer for longer, continuous-flow conditions, repeated electrochemical cycling, mixed microbial cultures, and complete microbial fuel cell performance, including power output.[12,33]

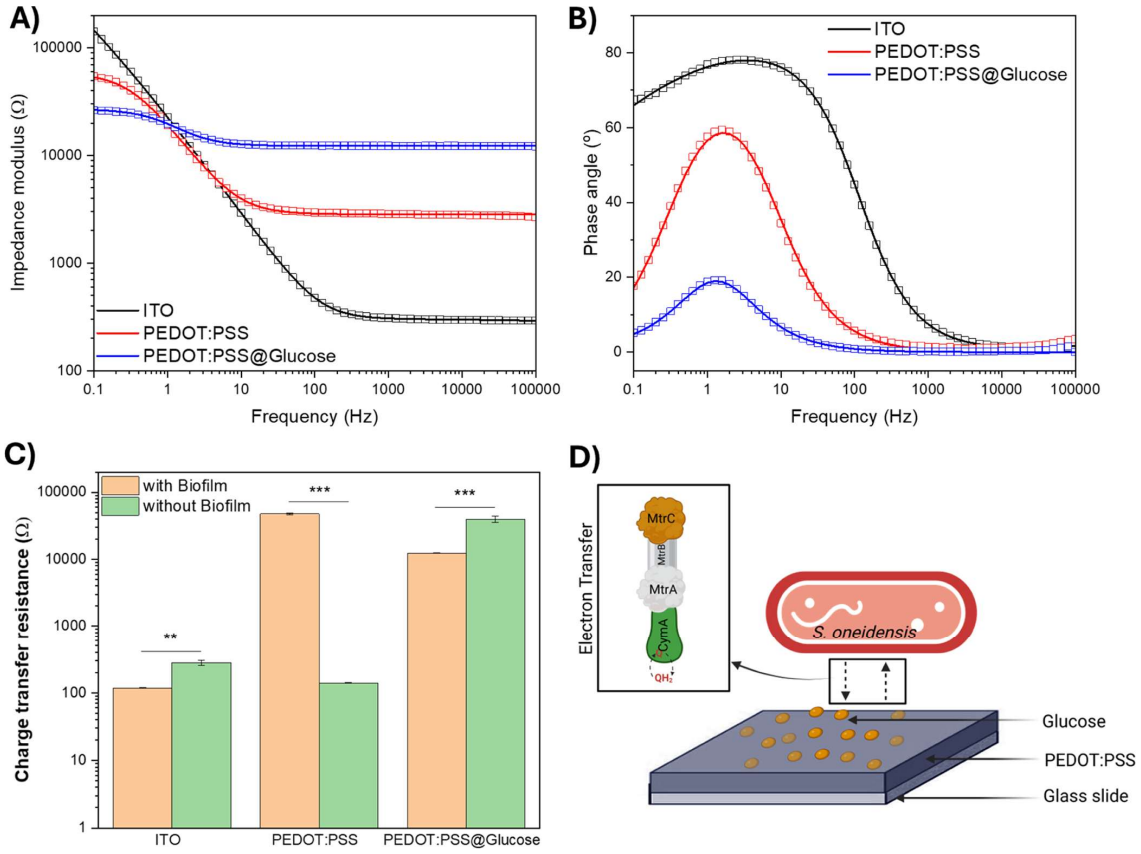



***Figure 6**: EIS response; frequency vs impedance (A), frequency vs phase angle (B), charge-transfer resistance (C), and proposed extracellular electron-transfer pathway for S. oneidensis on glucose-functionalized PEDOT:PSS (D). Reproduced from Figure 7 in [R2]. Copyright (2024) ACS Sustainable Chemistry & Engineering published by American Chemical Society.*

**In this chapter, I showed that a chemically simple secondary coating transformed PEDOT:PSS from a poorly colonized surface into a viable and electrochemically active microbial interface. Glucose provided the most effective balance between roughness, wettability, biological availability, and electrical coupling. The results also established an important methodological rule for the thesis: abiotic conductivity alone cannot predict the performance of a microbial electrode. Surface engineering should therefore be evaluated after biofilm formation, when bacterial physiology and extracellular electron transfer become active components of the system.**

## 4.3. Metal-ion-engineered PEDOT:PSS interfaces

### *4.3.1. Rationale for metal-ion functionalization*

The third publication advanced the surface engineering strategy by replacing organic modifiers with biologically relevant metal salts. PEDOT:PSS contains negatively charged sulfonate groups that can coordinate multivalent cations. I hypothesized that $Fe^{3+}$, $Mg^{2+}$, $Mn^{2+}$, $Ca^{2+}$, and $Ba^{2+}$ would alter PSS organization, screen surface charge, and change the distribution of PEDOT-rich electroactive domains. At the same time, several of these ions can influence *S. oneidensis* physiology, flavin secretion, autoaggregation, and biofilm formation [**R3**].[13,15] This approach therefore combined two mechanisms in a single procedure. At the material interface, the ions could induce ionic crosslinking, alter surface roughness and wettability, and influence charge storage properties. At the biological interface, they could modify cell surface interactions and affect microbial metabolism.

SEM images revealed that each metal ion produced a distinct surface morphology. Pristine PEDOT:PSS exhibited a smooth and homogeneous appearance at the micrometre scale. Iron functionalization developed a cracked, interconnected structure, whereas magnesium produced larger cracks separated by relatively smooth regions. Manganese resulted in fine irregular surface features, calcium produced a rough surface containing large aggregates, and barium formed pronounced crystalline structures as shown in **Figure 7**. EDS analysis confirmed the incorporation of the corresponding elements. After 24 h of immersion in PBS, $Fe^{3+}$, $Mg^{2+}$, $Mn^{2+}$, $Ca^{2+}$, and $Ba^{2+}$ remained detectable within the films, supporting at least partial coordination with PSS rather than simple superficial deposition.[13,38]

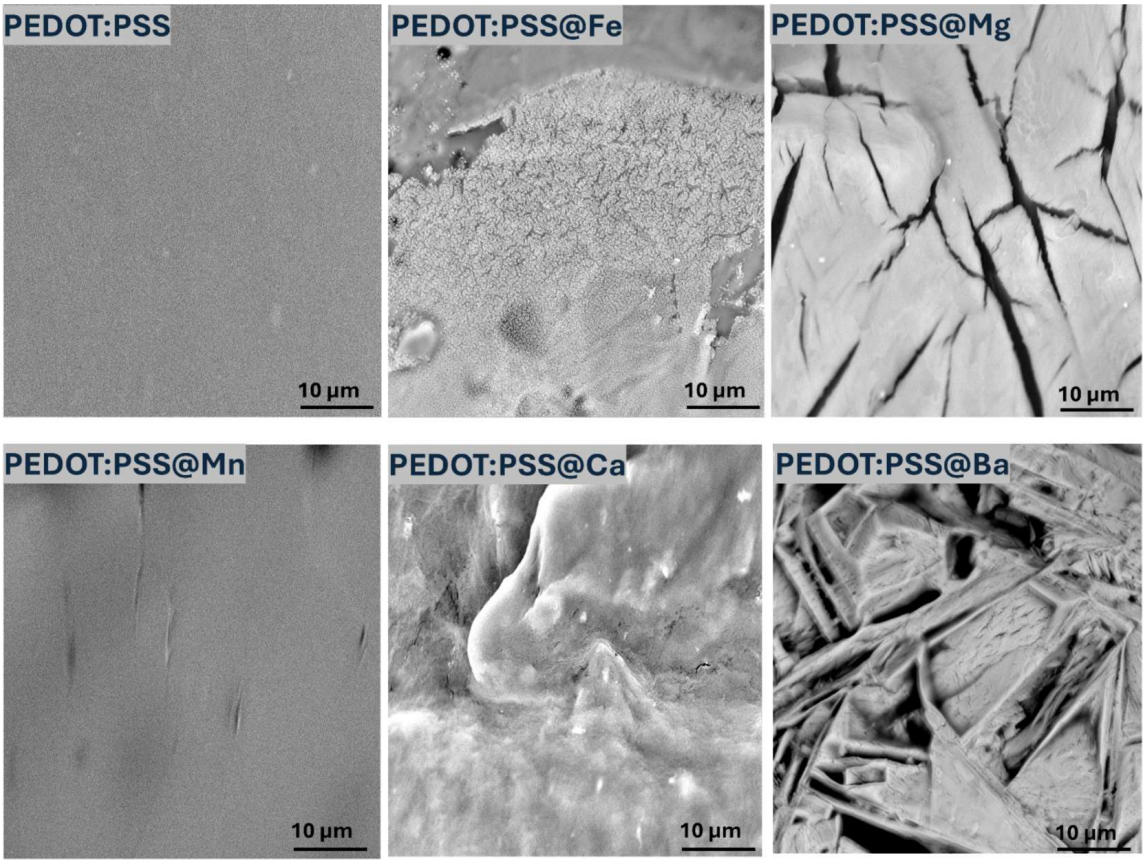



***Figure 7**: SEM images of pristine PEDOT:PSS and films modified with Fe, Mg, Mn, Ca, and Ba salts. Reproduced from Figure 1 in [R3]. Copyright (2025) Bioelectrochemistry published by Elsevier.*

### *4.3.2. Surface properties and chemical interactions*

Calcium produced the maximum increase in average roughness, from 1.1 ± 0.2 µm for pristine PEDOT:PSS to 3.6 ± 0.2 µm. Iron, magnesium, barium, and manganese produced intermediate values between approximately 1.7 and 2.0 µm. All metal-ion modifications increased hydrophilicity. The water contact angle decreased from 70.3 ± 0.6° as noted for pristine PEDOT:PSS to 36.5 ± 0.5° for PEDOT:PSS modified with calcium, 39.6 ± 0.9° for magnesium, 31.0 ± 0.5° for iron, 23.7 ± 1.1° for manganese, and 20.9 ± 2.0° for barium.[6,13]

FTIR spectra showed shifts in the S-O and S-phenyl bands of PSS and changes in PEDOT-associated C=C and C-S regions. The S-phenyl band near 1080 $cm^{-1}$ shifted to approximately 1046 $cm^{-1}$ for PEDOT:PSS@Ca. These changes support electrostatic

coordination between multivalent cations and sulfonate groups. Charge screening can reduce repulsion between PSS chains, compact the polymer chain, and permit closer packing or partial reorganization of PEDOT backbones. The observed morphology probably resulted from a combination of ionic coordination, PEDOT/PSS redistribution, and residual salt deposition during drying.[13,38]

Furthermore, the metal ion retention experiment was performed in PBS for assessing stability of the coatings. Calcium and iron showed substantial retention after immersion, whereas magnesium was detected at a lower concentration. This suggests that more strongly coordinating ions may penetrate or remain bound within PSS-rich domains more effectively. Some chloride-containing material also remained on the surfaces of the calcium and barium-treated samples, indicating that prolonged aqueous exposure may gradually alter the outermost morphology even when the coordinated cations remain associated with the polymer.[13,39]

### *4.3.3. Biofilm formation and viability*

The biological response was strongly metal-ion dependent. Pristine PEDOT:PSS supported only 4.1 ± 1.2% biofilm formation and 63.1 ± 7.2% viable cells. PEDOT:PSS@Ca produced the best overall result, with 55.0 ± 1.3% biofilm formation and 92.8 ± 3.1% viability. PEDOT:PSS@Mg supported 46.1 ± 1.4% biofilm formation and 99.6 ± 0.1% viability, while PEDOT:PSS@Fe produced 37.2 ± 1.3% biofilm formation and 95.9 ± 1.5% viability (**Figure 8A**, **B,** and **C**). PEDOT:PSS@Mn maintained very high viability but supported a few attached bacterial cells at its surface.[13,15]

Calcium is likely to act through both interfacial and biological mechanisms. Coordination with PSS may have reduced the negative charge of the polymer interface, thereby decreasing electrostatic repulsion between the surface and the negatively charged bacterial envelope. The increased surface roughness also provided additional sites for bacterial attachment. In parallel, calcium can promote cell autoaggregation, stabilize extracellular polymeric substances, and enhance riboflavin secretion. Together, these effects help explain why PEDOT:PSS@Ca supported both dense biofilm formation and high bacterial viability.[13,15] Barium produced the opposite outcome. PEDOT:PSS@Ba supported only 1.0 ± 0.9% biofilm formation and 43.1 ± 11.9% viability. The result

indicates that the surface can be highly rough and hydrophilic yet still exert an inhibitory effect. In this case, the specific chemistry of $Ba^{2+}$ and its influence on bacterial membrane function outweighed the potentially pro-adhesive effect of the surface morphology. This observation provided a direct conceptual link to the antibacterial coatings developed in the fifth publication.[13,40]

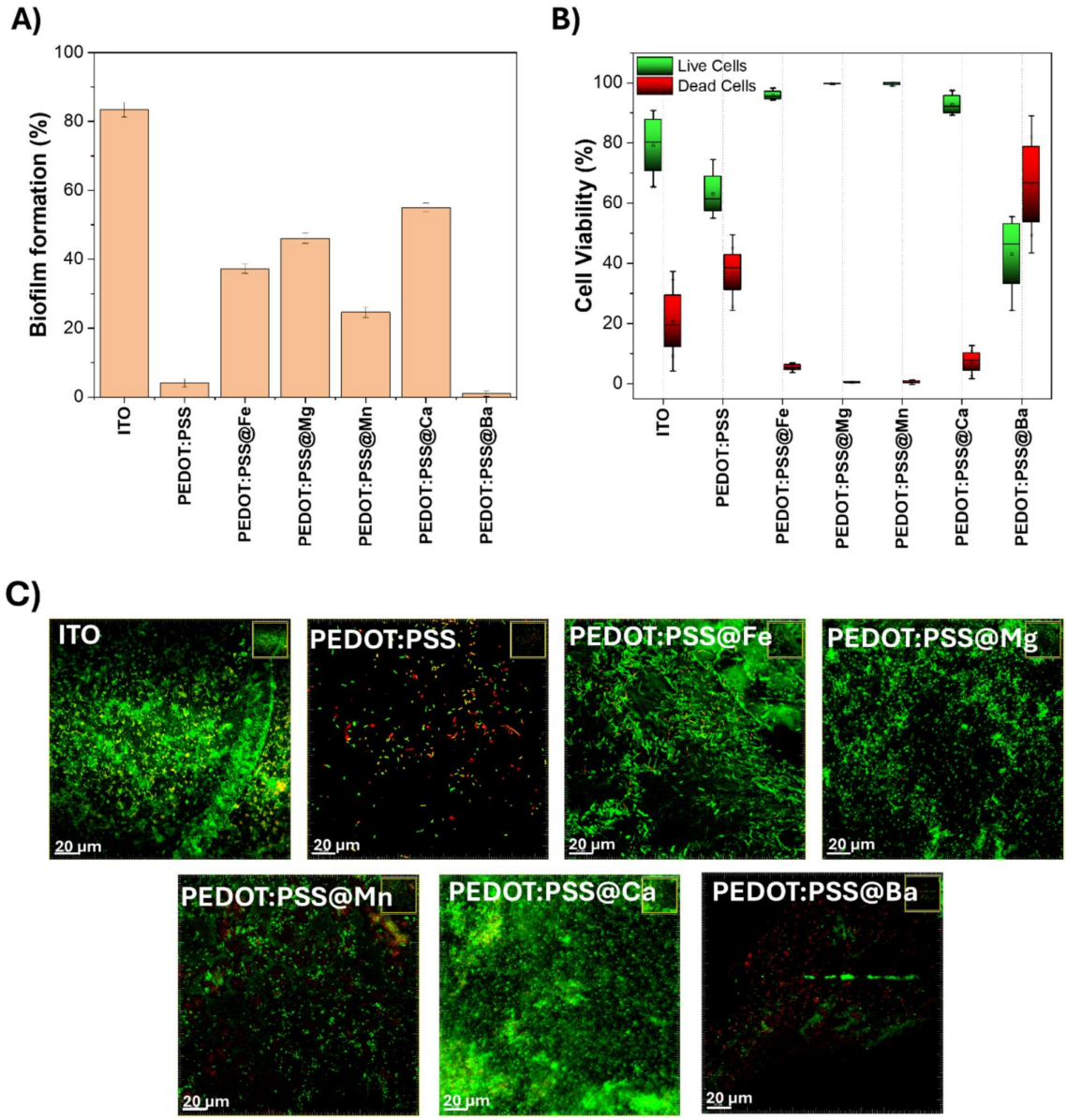



***Figure 8**: Biofilm formation (A), bacterial viability (B), and confocal LIVE/DEAD images of S. oneidensis on pristine and metal-ion-modified PEDOT:PSS films (C). Reproduced from Figure 4 in [R3]. Copyright (2025) Bioelectrochemistry published by Elsevier.*

### *4.3.4. Charge storage and interfacial resistance*

Cyclic voltammetry showed that $Ca^{2+}$, $Mn^{2+}$, and $Ba^{2+}$ produced the most pronounced changes in the electroactive behaviour of the films. Under abiotic conditions, the ion-modified coatings exhibited distinct oxidation and reduction currents, together with differences in stability during repeated potential cycling. These variations were consistent with ion exchange, partial leaching, and structural reorganization of PEDOT:PSS occurring during electrochemical cycling.[13,38]

The presence of *S. oneidensis* changed the interpretation. PEDOT:PSS@Ca reached a charge storage capacity of 5.1 ± 1.0 mC $cm^{-2}$ in the presence of the biofilm, representing an increase of approximately three orders of magnitude relative to the value obtained for pristine PEDOT:PSS under the same biological conditions (**Figure 9A**, **B**). PEDOT:PSS@Fe also showed a substantial improvement. The result reflected the combined contribution of the modified polymer, the viable biofilm, outer-membrane cytochromes, and flavin-mediated charge exchange.[13,41]

EIS supported this conclusion. In the presence of *S. oneidensis*, PEDOT:PSS@Ca exhibited a charge-transfer resistance of 834 ± 84 Ω, while PEDOT:PSS@Fe showed Rct of 3.80 ± 0.26 kΩ. Calcium therefore produced the most effective interface. The reduced resistance cannot be attributed only to a more conductive abiotic film; it is consistent with improved cell attachment, closer cytochrome contact, and a hydrated ion-rich pathway for electron mediator exchange.[13,20] These results also reveal that a coating may display a large capacitive response because of ion movement or mediator redox cycling while still having a relatively high Rct. For microbial electrode design, both parameters should be considered together with biofilm density and viability.[13,41]

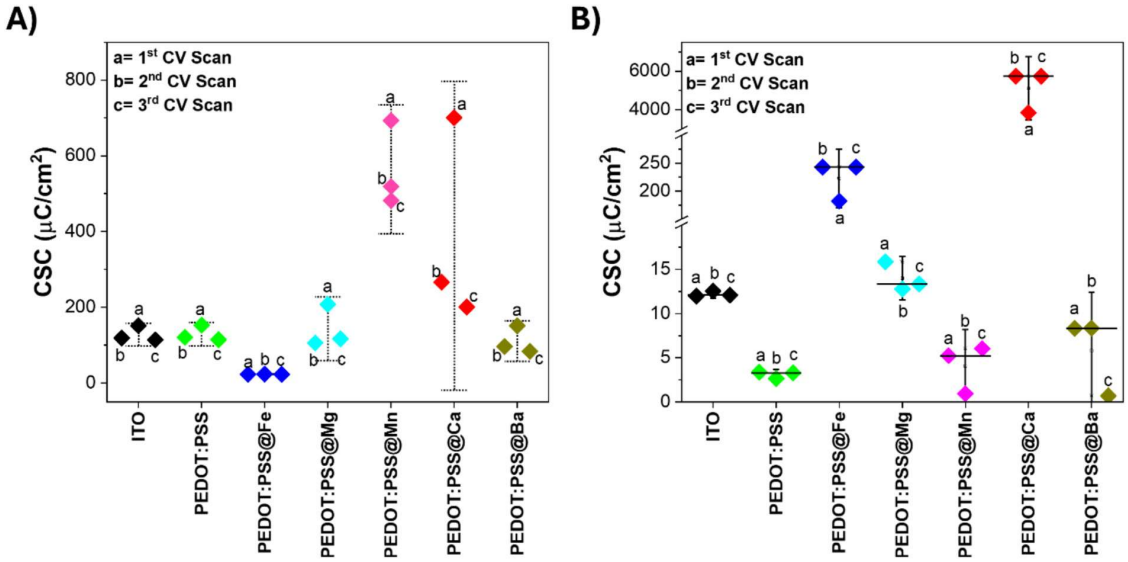



***Figure 9**: Charge storage capacity of pristine and metal-ion-modified PEDOT:PSS under abiotic conditions (A) and after S. oneidensis biofilm formation (B). Reproduced from Figure 6 in [R3]. Copyright (2025) Bioelectrochemistry published by Elsevier.*

### *4.3.5. Significance and limitations*

This study identified calcium as the most effective modifier for *S. oneidensis* based microbial electrodes, whereas barium emerged as a potential route toward antibacterial PEDOT:PSS interfaces. This contrast is scientifically important because it demonstrates that the identity of the incorporated ion can direct the same polymer platform toward fundamentally different biological functions. The modification strategy is also experimentally simple, compatible with flexible electrode substrates, and does not require the synthesis of a new polymer.[13]

The main limitations concern long-term ion stability, concentration gradients, and biological specificity. Although EDS confirmed ion retention after 24 h, loosely bound salts may continue to leach during prolonged operation. Further studies should therefore include depth-resolved elemental analysis, direct conductivity measurements, and long-term microbial fuel cell experiments. The biological response should also be evaluated in defined media and mixed microbial communities, as nutrient-rich LB medium may mask the specific effects of the incorporated ions or nutrient availability.[13,39]

**In this chapter, I showed that metal ions acted both as material modifiers and as biological regulators at PEDOT:PSS interfaces. Calcium provided the most favourable combination of surface roughness, wettability, biofilm formation, bacterial viability, charge-storage capacity, and low interfacial resistance. In contrast, barium shifted the same polymer platform toward an antibacterial response. These findings expanded the thesis from organic surface functionalization to ionic control and confirmed that relatively small chemical changes at the interface can substantially alter both bacterial behaviour and electrochemical performance.[13]**

## 4.4. Surfactant-doped PEDOT antibacterial coatings

### *4.4.1. Concept and electropolymerization*

The fourth publication shifted the objective of the interface from promoting electroactive biofilm formation to preventing bacterial colonization on biomedical devices. Medical and bioelectronic devices require coatings that maintain electrochemical functionality while resisting infection-associated biofilm development. DTAB was selected because its quaternary ammonium headgroup can interact electrostatically with negatively charged bacterial envelopes, whereas its dodecyl chain can penetrate lipid membranes and disrupt membrane integrity and permeability [**R4**].[14,40]

PEDOT and PEDOT@DTAB were electropolymerized on flexible ITO/PET (**Figure 10A, B**). DTAB improved the dispersion of EDOT in PBS and acted as a structure-directing species during polymer growth. The polymerization currents were substantially larger in the presence of DTAB, and the reduction peak shifted during successive scans, indicating progressive incorporation of the surfactant into the developing matrix (**Figure 10C**, **D**). FTIR and EDS later confirmed this incorporation through alkyl-chain vibrations and the presence of nitrogen and bromine.[14,38]

The resulting coating was designed to perform three functions simultaneously. PEDOT provided reversible redox activity and charge storage. The incorporated surfactant altered polymer morphology and ion exchange. Finally, DTAB acted as a membrane-active antibacterial agent that could be released passively or by electrical stimulation.[14,24]

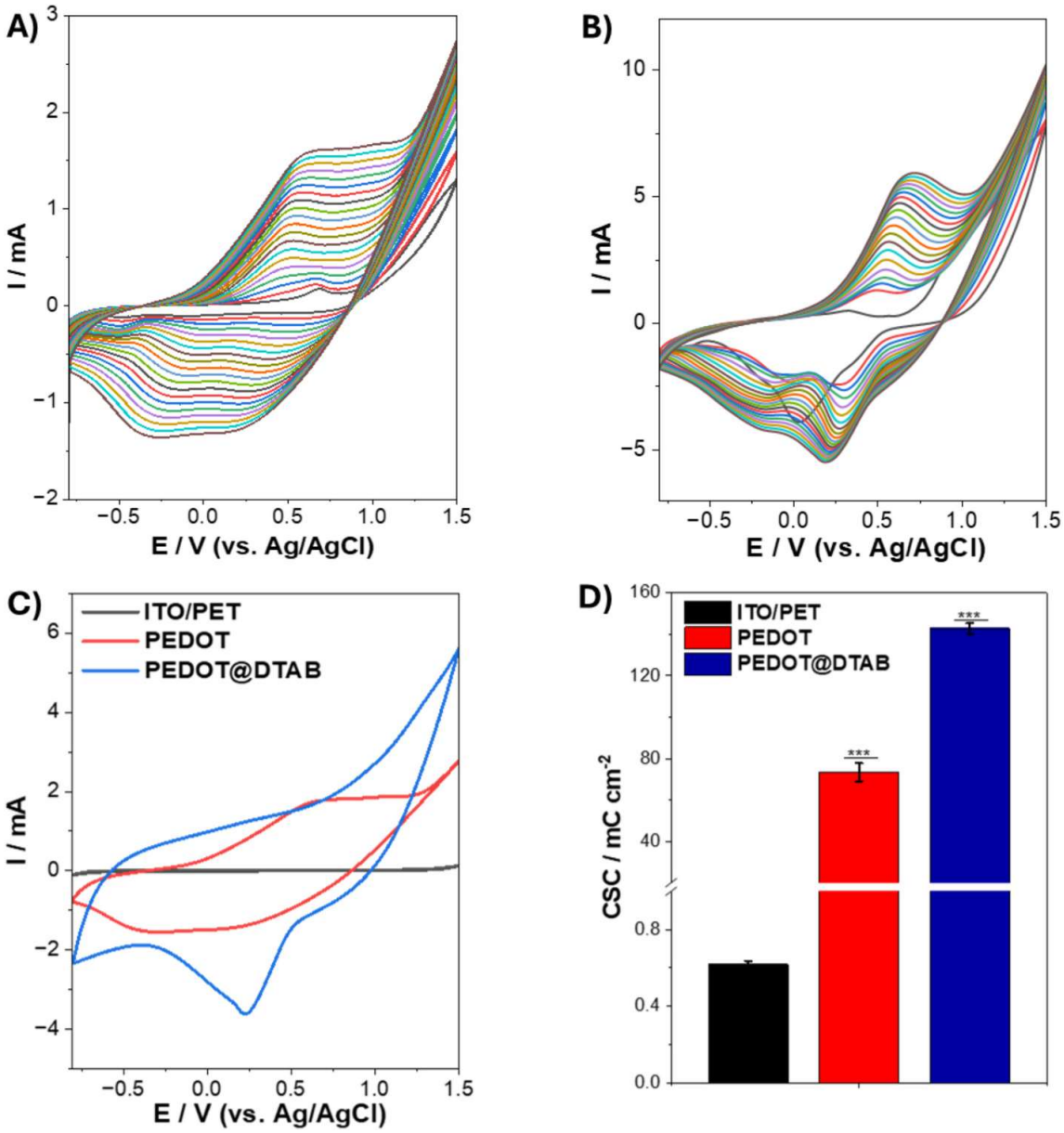



***Figure 10**: Electropolymerization of PEDOT (A), and PEDOT@DTAB (B), cyclic voltammetry of the resulting films (C), and calculated charge storage capacity (D). Reproduced from Figure 1 in [R4]. Copyrights (2026) Bioelectrochemistry published by Elsevier.*

### *4.4.2. Electrochemical and surface properties*

PEDOT@DTAB exhibited a much larger cyclic voltammetry area than pristine PEDOT (**Figure 10C**). The charge storage capacity increased from 73.4 ± 4.3 mC $cm^{-2}$ for PEDOT to 142.7 ± 2.5 mC $cm^{-2}$ for PEDOT@DTAB, corresponding to an improvement of approximately 94% (**Figure 10D**). The enhanced CSC is consistent with

surfactant-assisted formation of an open electroactive structure and more extensive reversible ion exchange during doping and dedoping.[14,38]

At the same time, EIS revealed a pronounced increase in charge-transfer resistance. Rct increased from 292 ± 26 Ω for PEDOT to 17.9 ± 0.3 kΩ for PEDOT@DTAB. The coating therefore stored more charge but allowed slower interfacial charge transfer. This result is characteristic of a capacitive, partially blocking film: ions can be accumulated and released throughout the polymer, while direct faradaic exchange across the outer interface is hindered by the surfactant-rich structure.[14,19]

Surface roughness remained close to 2 µm for both PEDOT and PEDOT@DTAB, indicating that roughness was not the principal source of the antibacterial difference. Wettability changed more strongly. The water contact angle decreased from 82.3 ± 2.5° for ITO/PET to 11.6 ± 1.2° for PEDOT and to 5.4 ± 0.5° for PEDOT@DTAB. The nearly superhydrophilic character of the modified film supports rapid contact with aqueous media, while the immobilized cationic headgroups and hydrophobic chains retain membrane-disruptive functionality.[5,14]

### *4.4.3. Passive and electrically triggered release*

Under passive conditions, DTAB was released slowly from PEDOT@DTAB. The cumulative amount increased from approximately 0.6 ± 0.1 µg $cm^{-2}$ at the first measurement (0.5 h) to 30.6 ± 3.4 µg $cm^{-2}$ after 24 h (**Figure 11A**, **B**). The gradual release profile indicated that a considerable fraction of the surfactant was retained by physical entrapment, electrostatic interactions, and limited swelling of the PEDOT matrix.[14,42]

The passive profile fitted the Higuchi model with $R^2 = 0.99$, confirming a strong diffusion contribution (**Figure 11C**). The Korsmeyer-Peppas exponent was approximately 1.04 in the initial region, indicating that diffusion alone was not sufficient to describe the process. Polymer relaxation, swelling, reorganization, and ion exchange also contributed to DTAB transport.[43,44]

Electrical stimulation produced a much faster and larger release. Repeated cyclic-voltammetry scans between -0.6 V and +0.6 V vs. Ag/AgCl increased the cumulative DTAB release amount from 25.5 ± 2.4 µg $cm^{-2}$ after five CV cycles to 79.1 ± 5.5 µg $cm^{-2}$ after 160 CV cycles (**Figure 11D**, **E**). Approximately one third of the final amount was

released within the first short stimulation period. The active process was therefore best described as an electrically triggered burst followed by diffusion-controlled transport (**Figure 11F**).[14,24]

The mechanism is linked to redox switching of PEDOT. Oxidation and reduction cause chain expansion and contraction, counter-ion movement, and changes in electrostatic interaction between the polymer and DTAB. These changes accelerated the release of the cationic surfactant. Minor swelling and peeling began after the highest stimulation level, defining 160 CV cycles as the practical stability limit under the tested conditions.[24,45]

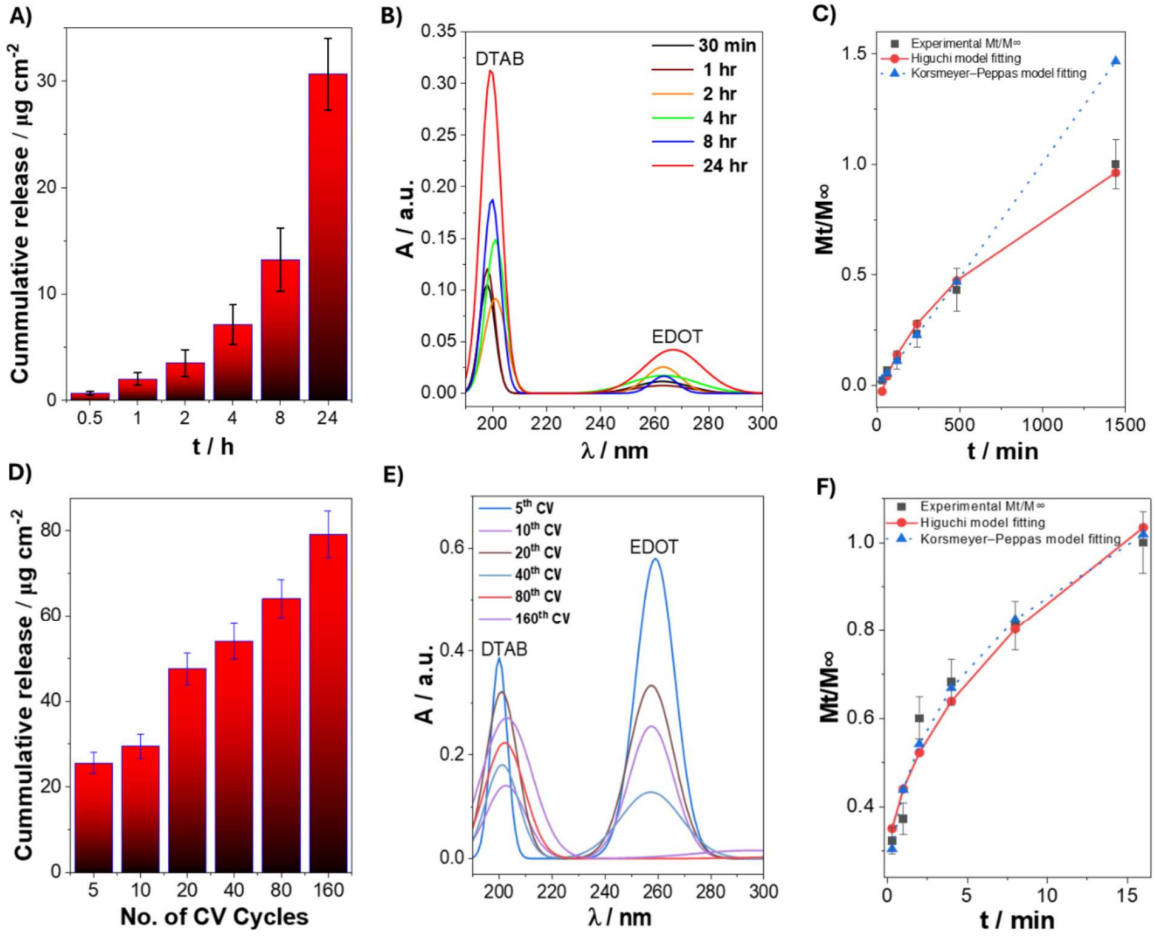



***Figure 11**: Passive drug release (A), its UV-Vis confirmation (B), kinetic-model fitting (C). Electrically triggered DTAB release (D), its UV-Vis confirmation (E), and kinetic-model fitting (F). Reproduced from Figure 5 in [R4]. Copyrights (2026) Bioelectrochemistry published by Elsevier.*

### *4.4.4. Antibacterial and antibiofilm activity*

Free DTAB inhibited both bacterial species in a concentration-dependent manner. The calculated $MIC_{50}$ was 90.3 μg $mL^{-1}$ for *S. oneidensis* and 174.5 μg $mL^{-1}$ for *P. aeruginosa*, confirming the greater intrinsic resistance of *P. aeruginosa*. The difference is consistent with species-specific membrane composition, efflux, and stress-response mechanisms.[14,46]

PEDOT@DTAB inhibited biofilm formation by 95.4 ± 2.2% for *S. oneidensis* and 45.7 ± 2.1% for *P. aeruginosa* (**Figure 12A**). LIVE/DEAD microscopy showed that *S. oneidensis* viability decreased from 92 ± 2% on ITO/PET to 62 ± 6% on PEDOT and 21 ± 8% on PEDOT@DTAB (**Figure 12B, D**). For *P. aeruginosa*, the corresponding values were 95 ± 3%, 69 ± 4%, and 60 ± 6%, respectively (**Figure 12C, E**). Thus, PEDOT@DTAB exhibited a strong antibacterial effect against *S. oneidensis*, while its effect on *P. aeruginosa* was more moderate.[14,28]

The antibacterial activity likely involved both release-mediated and contact-dependent mechanisms. Positively charged ammonium groups can electrostatically attract the negatively charged bacterial envelope, promoting close interaction between the cell surface and the coating. The dodecyl chain can then penetrate the lipid region, increase permeability, and cause leakage of cellular contents. The local interfacial concentration can be biologically effective even when the average amount released into the bulk medium is below the measured $MIC_{50}$. This explains why the coating inhibited *P. aeruginosa* despite its higher resistance to free DTAB.[14,46]

Long-term measurements showed that growth inhibition remained 73.0 ± 0.6% for *S. oneidensis* and 44.5 ± 0.1% for *P. aeruginosa* after seven days. Scratch testing also demonstrated stronger mechanical resistance. The first and major damage loads increased from 65.2 mN and 183.5 mN for PEDOT to 236.8 mN and 323.6 mN for PEDOT@DTAB. DTAB incorporation therefore improved not only biological performance but also resistance to mechanical damage.[14,18]

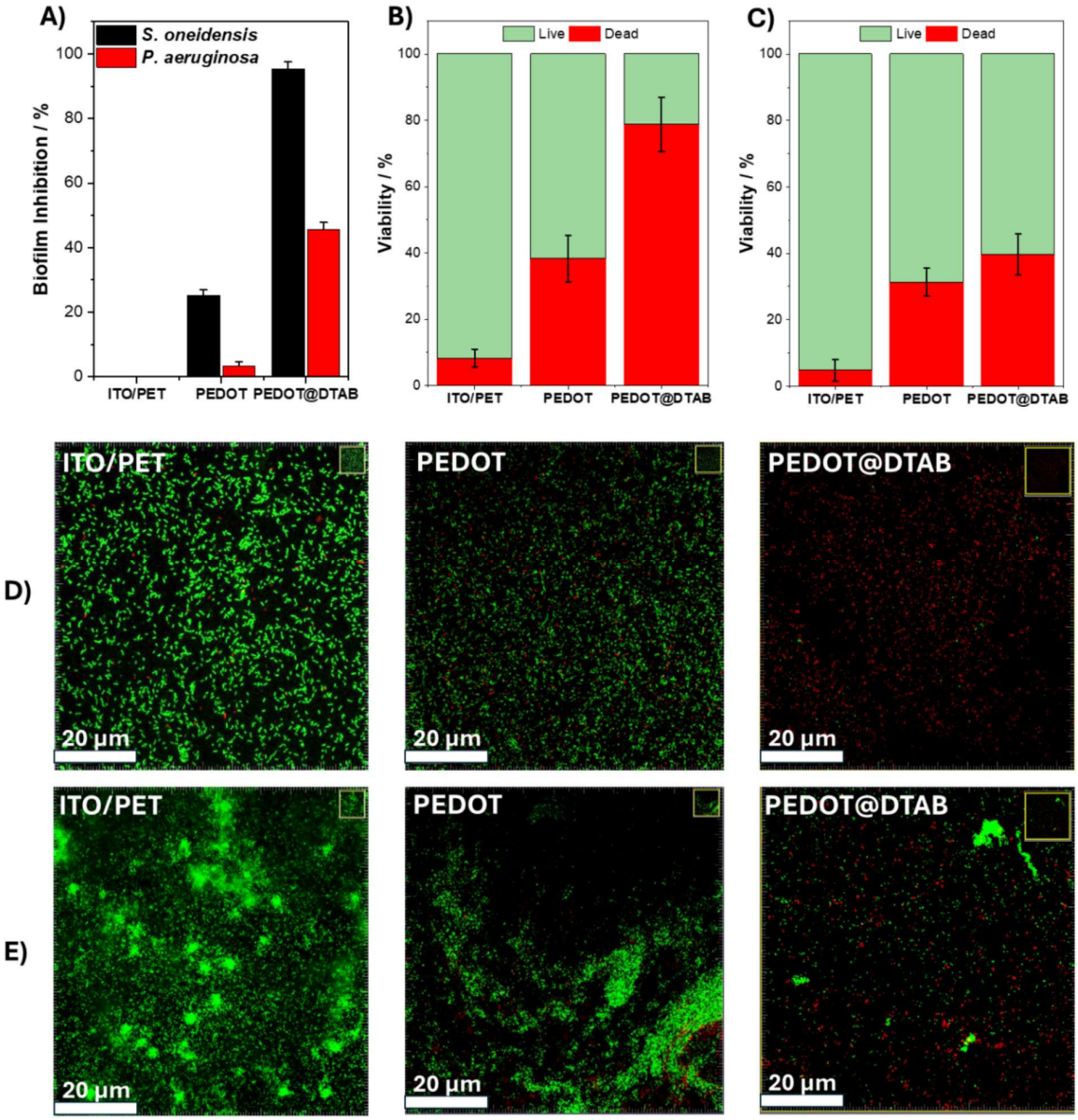



***Figure 12**: Biofilm inhibition (A), bacterial viability for S. oneidensis (B) and P. aeruginosa (C), and confocal LIVE/DEAD images of S. oneidensis (D) and P. aeruginosa (E) on ITO/PET, PEDOT, and PEDOT@DTAB. Reproduced from Figure 6 in [R4]. Copyrights (2026) Bioelectrochemistry published by Elsevier.*

### *4.4.5. Species-dependent electrochemical behaviour and significance*

The electrochemical response of the bacterial films was species dependent. In the presence of *S. oneidensis*, PEDOT@DTAB showed a lower charge-storage response than pristine PEDOT, consistent with reduced attachment and disruption of direct cytochrome-based coupling. *P. aeruginosa* produced a larger capacitive response because secreted

phenazines could undergo redox cycling even when direct bacterial contact was limited. Nevertheless, the Rct remained high, indicating that the temporary increase in mediator-driven charge storage did not translate into efficient long-range charge transfer across the surfactant-rich interface.[4,14]

This distinction is central to the interpretation of smart antibacterial coatings. A high current response or large CSC in the presence of bacteria does not necessarily indicate the formation of an active, electrically conductive biofilm. Instead, it may reflect redox cycling of soluble mediators near an otherwise charge-transfer-limiting interface. By combining cyclic voltammetry, electrochemical impedance spectroscopy, biofilm quantification, and bacterial viability analysis, these different contributions could be distinguished more reliably.[14,40]

The main limitations of this part of my studies include the potential cytotoxicity of quaternary ammonium compounds toward mammalian cells, the finite loading capacity of DTAB within the coating, and possible structural changes following repeated electrical stimulation. Future studies should therefore focus on optimizing the surfactant concentration, evaluating the stability and reproducibility of repeated release cycles, testing the coatings under physiologically relevant conditions in the presence of serum proteins, and assessing cytocompatibility with appropriate eukaryotic cell models. The use of more targeted antibacterial agents or bacteria-responsive redox triggers may further improve the selectivity of these systems.[14,40]

**In this chapter, I developed a dual-function PEDOT coating that combined high charge-storage capacity with electrically tunable antibiofilm activity. DTAB served simultaneously as a dopant, a structure-directing component, and a releasable antibacterial agent. The species-dependent responses of *S. oneidensis* and *P. aeruginosa* further demonstrated that electrochemical behaviour must be interpreted in the context of the complete biological interface. This study completed the progression of the thesis from promoting beneficial microbial electron transfer to actively suppressing undesirable bacterial colonization on conducting-polymer-based surfaces.**[14,24]

## 4.5. Bacteria-responsive ceftazidime-loaded PEDOT coatings

### *4.5.1. Position of the main manuscript within the thesis*

The development of the PEDOT@CAZ interface is the main experimental study of this dissertation because it combined the surface, electrochemical, microbiological, and release concepts developed in the preceding chapters. The earlier work showed that bacterial behaviour at a PEDOT interface can be altered by organic modifiers, metal ions, and surfactant dopants. It also showed that electroactive bacteria can exchange electrons with conducting polymers and could measurably change interfacial capacitance and resistance. I used this understanding to ask a more demanding question. Could the electrical activity of bacteria be converted into a therapeutic signal, so that an antibiotic is retained under normal conditions and released when an electroactive biofilm begins to interact with the coating?[9]

Ceftazidime was selected as the model antibiotic because it is effective against Gram-negative organisms, including *P. aeruginosa*, and contains several heteroatoms and functional groups capable of interacting with PEDOT during electropolymerization. The design did not rely on covalent drug attachment. Instead, CAZ was introduced into the EDOT dispersion and incorporated during film growth, allowing the drug to remain accessible to redox-driven ion exchange and polymer rearrangement. This choice was deliberate: a covalent linkage might improve retention but could also suppress release or reduce antibiotic activity. The resulting material was therefore expected to balance three competing requirements: sufficient drug loading, limited passive leakage, and responsiveness to redox activity at the bacteria-material interface [**R5**].[26,27]

Two electroactive bacteria were used to test this concept. *S. oneidensis* transfers electrons through outer-membrane cytochromes and secreted flavins, whereas *P. aeruginosa* relies strongly on phenazine metabolites and additional conductive structures. Their different extracellular electron-transfer pathways provided a useful test of whether release was simply caused by bacterial growth or was related to the way each organism interacted electrochemically with PEDOT. *S. aureus*, *E. coli*, and pH-adjusted sterile media were included as controls to strengthen this distinction.[34,35]

### *4.5.2. Electropolymerization and electrochemical properties of PEDOT@CAZ*

PEDOT and PEDOT@CAZ were electropolymerized on flexible ITO/PET electrodes by cycling the potential between -0.8 V and +1.5 V vs. Ag/AgCl. The progressive increase in anodic and cathodic current during successive cycles confirmed continued film growth. CAZ did not prevent polymer formation, but it changed the redox response of the final coating. Pristine PEDOT showed oxidation and reduction features close to +0.2 V and -0.2 V (**Figure 13A**), while the oxidation feature of PEDOT@CAZ shifted toward approximately +0.6 V (**Figure 13B**). Because free CAZ oxidized at a substantially more positive potential, this shift was interpreted as a change in the local electronic environment of PEDOT rather than a direct superposition of the antibiotic peak. Electrostatic, hydrogen-bonding, and other chemical interactions between CAZ and the growing polymer chains most likely altered chain packing and, consequently, the charge required for polymer oxidation.[38,47]

The incorporation of CAZ did not significantly reduce the amount of reversible charge stored by the polymer. The CSC of PEDOT@CAZ was 14.6 ± 3.4 mC $cm^{-2}$, compared with 11.2 ± 2.8 mC $cm^{-2}$ for pristine PEDOT (**Figure 13C**). Both values were substantially higher than the 34.8 ± 4.7 μC $cm^{-2}$ measured for bare ITO/PET. This finding was particularly important for the intended application. Despite the incorporation of a relatively large and poorly conducting molecule within the polymer matrix, the coating retained the charge-storage capacity required for effective redox switching.[1,48]

Impedance measurements revealed the complementary effect of drug loading. The charge-transfer resistance increased from 81 ± 9 Ω for ITO/PET to 494 ± 38 Ω after PEDOT deposition and to 10.7 ± 0.5 kΩ after CAZ incorporation (**Figure 13D, E**). The increase was not interpreted as evidence of poor polymerization. Instead, it indicated that CAZ introduced localized insulating regions, disrupted the conjugated polymer network, and restricted ion and electron transport across the interface. The high resistance and preserved CSC together describe a coating that stores charge efficiently but releases it through a more spatially heterogeneous pathway. This combination later proved relevant to both controlled release and species-dependent bacterial responses.[19,49]

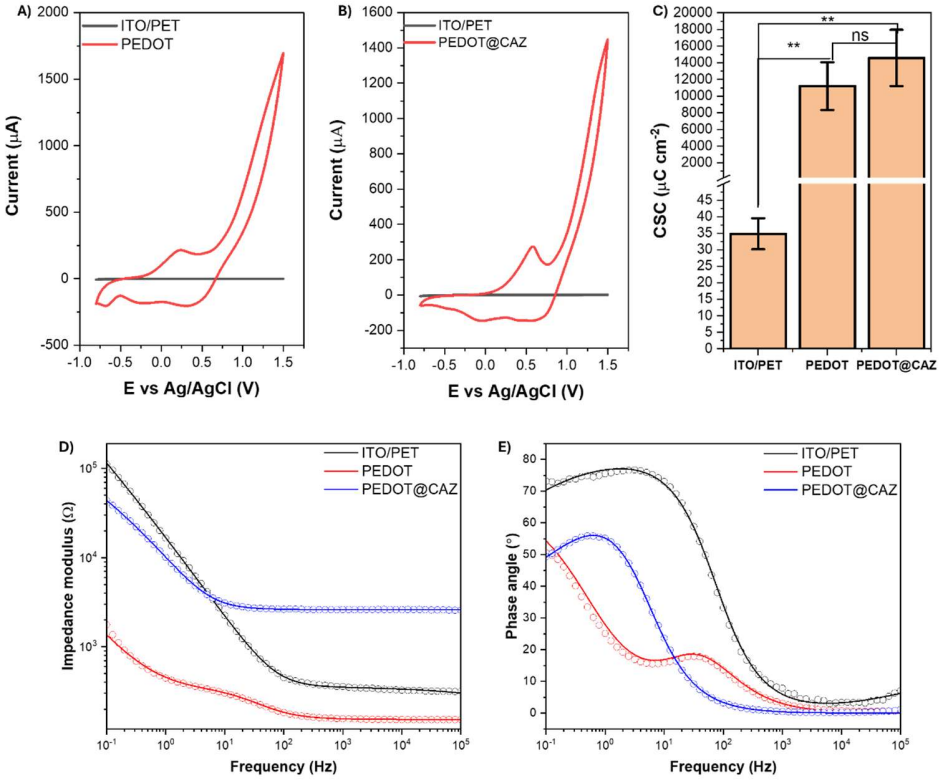



***Figure 13**: Cyclic voltammetry of PEDOT (A) and PEDOT@CAZ (B), charge-storage capacity (C), and impedance response; frequency vs. impedance (D), frequency vs. phase angle (E) of ITO/PET, PEDOT, and PEDOT@CAZ. Adapted from Figure 1 in [R5]. Copyrights (2026) Advanced Materials Interfaces published by Wiley-VCH GmbH.*

### *4.5.3. Chemical incorporation, morphology, and surface properties*

FTIR spectroscopy provided direct evidence that CAZ remained in the polymer after electropolymerization and rinsing. Free CAZ exhibited a broad N-H-associated band at 3460 $cm^{-1}$, whereas the corresponding feature in PEDOT@CAZ was stronger and shifted to 3305 $cm^{-1}$. The beta-lactam carbonyl band shifted from 1752 $cm^{-1}$ in CAZ to approximately 1730 $cm^{-1}$ in the composite. Several additional CAZ bands remained visible with changes in intensity or position (**Figure 14A**). At the same time, the characteristic PEDOT bands, including the thiophene C=C vibration near 1516 $cm^{-1}$ and the ethylenedioxy-associated bands, were retained. The spectra therefore support non-covalent incorporation rather than chemical destruction of either component.[23,50]

EDS reinforced this conclusion. Nitrogen was absent from pristine PEDOT but accounted for 8.91 wt.% of the PEDOT@CAZ film. Because nitrogen is abundant in the

beta-lactam, amide, and aminothiazole groups of CAZ (**Figure 14B**), its appearance after extensive rinsing is a clear marker of drug retention. The simultaneous detection of carbon, oxygen, and sulfur from PEDOT and nitrogen from CAZ confirmed that the film was a composite rather than a simple surface deposit.[9,23]

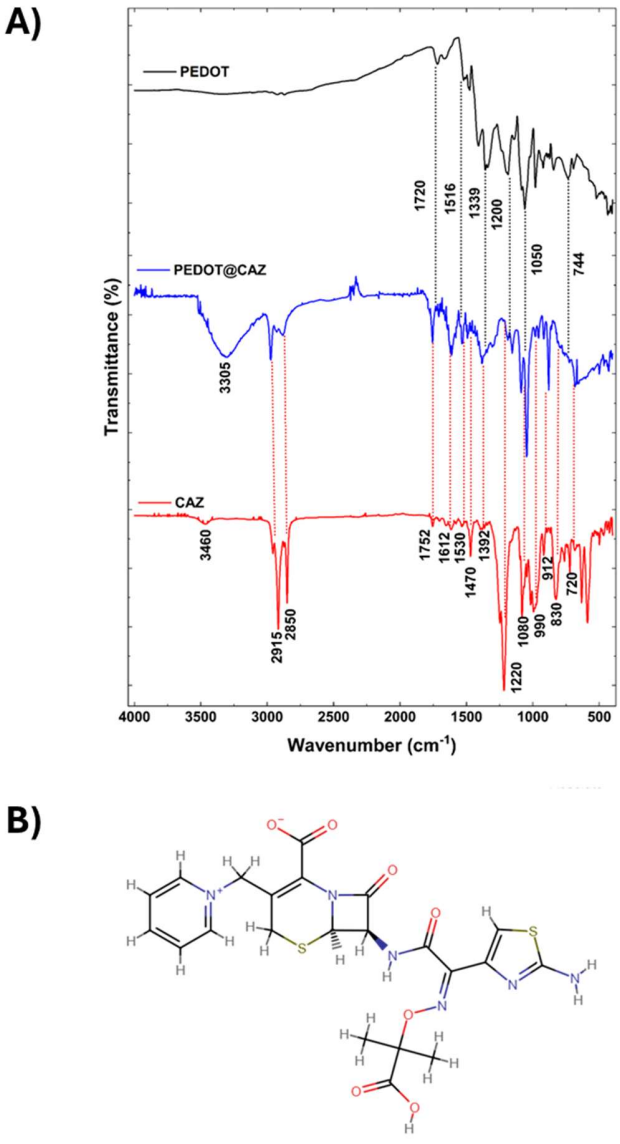



***Figure 14**: FTIR spectra of PEDOT, PEDOT@CAZ, and ceftazidime (A), together with the molecular structure of CAZ (B). Adapted from Figure 2 in [R5]. Copyrights (2026) Advanced Materials Interfaces published by Wiley-VCH GmbH.*

The PEDOT morphology changed visibly after drug incorporation. Pristine PEDOT formed a densely packed granular network (**Figure 15A**). PEDOT@CAZ contained larger and less regular spherical aggregates, consistent with local interruption of polymer growth by the bulky antibiotic (**Figure 15B**). The change created a more heterogeneous and porous surface without causing a statistically significant increase in average roughness beyond that of PEDOT. Bare ITO/PET had a roughness of 0.40 ± 0.10 µm; PEDOT and PEDOT@CAZ reached 1.96 ± 0.40 µm and 2.10 ± 0.50 µm, respectively (**Figure 15C**).[48,51] Both polymer coatings were strongly hydrophilic. The water contact angle decreased from 82.0 ± 2.5° for ITO/PET to 11.0 ± 1.2° for PEDOT and 12.0 ± 0.9° for PEDOT@CAZ (**Figure 15D**).

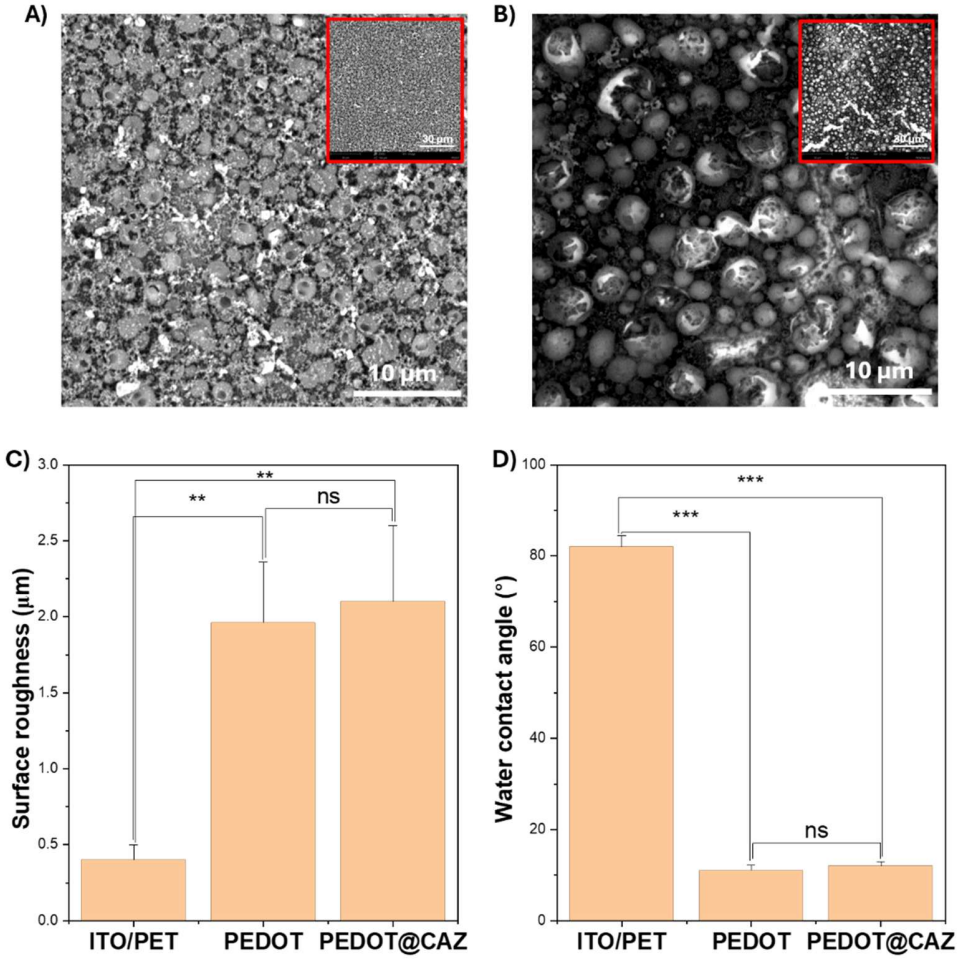



***Figure 15**: SEM morphology of PEDOT (A), and PEDOT@CAZ (B). Surface roughness (C), and water contact angle of ITO/PET, PEDOT, and PEDOT@CAZ (D). Adapted from Figure 3 in [R5]. Copyrights (2026) Advanced Materials Interfaces published by Wiley-VCH GmbH.*

### *4.5.4. Passive, electrically stimulated, and bacteria-triggered CAZ release*

The release experiments were designed to separate three modes of transport. Passive release measured the amount lost from the coating without an applied potential or bacterial stimulus. Electrically stimulated release established the maximum response that could be produced by deliberate redox cycling. Bacteria-triggered release then tested whether microbial electron transfer could generate a comparable drug release effect without an external power source.[24,45]

Passive leakage was found to be low. PEDOT@CAZ released 0.44 ± 0.01 μg $cm^{-2}$ CAZ after 5 min and 0.50 ± 0.01 μg $cm^{-2}$ CAZ after 30 min. The cumulative release value increased to only 1.2 ± 0.1 μg $cm^{-2}$ after 60 min (**Figure 16A**). The early fraction was attributed mainly to loosely associated CAZ near the coating surface, while the later increase reflected slower diffusion from deeper regions. The absence of a large burst was favourable because premature loss would shorten the lifetime of the coating and expose surrounding tissue to antibiotic in the absence of infection.[48,52]

Electrical cycling produced a markedly different profile. The first five CV cycles released 8.2 ± 1.8 μg $cm^{-2}$ CAZ, and the cumulative CAZ amount increased to 21.3 ± 3.3 μg $cm^{-2}$, 29.6 ± 4.2 μg $cm^{-2}$, 37.9 ± 5.3 μg $cm^{-2}$, and 49.5 ± 5.9 μg $cm^{-2}$ after 15, 30, 60, and 120 CV cycles, respectively (**Figure 16B**). The progressive increase in charge passed through the coating is consistent with repeated doping and dedoping, counter-ion exchange, polymer swelling, and chain rearrangement. Beyond 120 CV cycles, however, minor delamination was observed, indicating that the stimulation protocol had reached the practical stability limit of the coating rather than a desirable operating condition for controlled release.[24,45]

The most important result was obtained after 24 h exposure to bacteria. *S. oneidensis* triggered CAZ release of 44.4 ± 9.0 μg $cm^{-2}$, while *P. aeruginosa* triggered CAZ release of 62.2 ± 2.8 μg $cm^{-2}$ (**Figure 16C**). The quantity of CAZ released was greater than that achieved through vigorous external cycling and was significantly higher than the passive release level. The greater release observed in the presence of *P. aeruginosa* was consistent with the production of diffusible phenazines, which can act as redox mediators and shuttle electrons between bacterial cells and the polymer. In contrast, *S. oneidensis* relies more strongly on cytochromes, flavins, and contact-associated electron-transfer pathways, resulting in a different pattern of redox perturbation at the interface.[34,35]

Control experiments were necessary because bacterial growth can alter pH, consume nutrients, and generate a wide range of metabolites, any of which could influence the observed release behaviour. *S. aureus* and *E. coli* caused only 3.0 ± 0.5 µg $cm^{-2}$ and 1.5 ± 0.4 µg $cm^{-2}$ release of CAZ, respectively. Sterile LB adjusted to pH 5.5 or 8.5 produced no detectable CAZ peak. These findings do not demonstrate that extracellular electron transfer is the sole mechanism responsible for drug release; however, they indicate that bacterial growth or pH changes alone cannot explain the substantial release observed in the presence of electroactive bacteria. I therefore described the coating as bacteria-redox-responsive, while acknowledging that further mechanistic studies are required to define the specific contributions of individual redox pathways.[53,54]

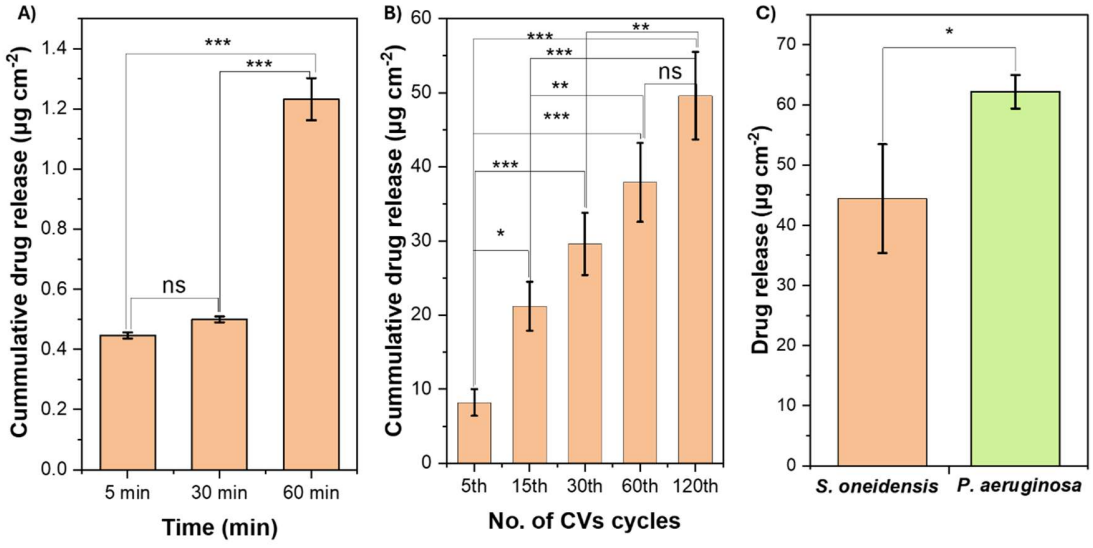



***Figure 16**: Passive drug release (A), electrically triggered drug release (B), and bacteria-triggered ceftazidime release from PEDOT@CAZ (C). Adapted from Figure 4 in [R5]. Copyrights (2026) Advanced Materials Interfaces published by Wiley-VCH GmbH.*

### *4.5.5. Species-dependent electrochemical interaction with the coating*

The cyclic voltammograms recorded after bacterial incubation with the coating confirmed that the two species interacted with the electrodes in different ways. *S. oneidensis* produced broad, mainly capacitive responses without sharply resolved redox peaks (**Figure 17A)**. In this case, PEDOT@CAZ reached a CSC of 643 ± 51 µC $cm^{-2}$, compared with 124 ± 14 µC $cm^{-2}$ for PEDOT and 36 ± 9 µC $cm^{-2}$ for ITO/PET (**Figure**

**17B**). The enlarged voltammetric area is consistent with charge storage in the polymer-biofilm composite and with flavin or cytochrome-mediated exchange that is distributed over a range of potentials rather than concentrated in a single reversible couple.[36,41]

*P. aeruginosa* generated clear reduction and oxidation peaks between approximately -0.5 and -0.2 V (**Figure 17C**). These peaks are characteristic of phenazine-mediated electron transfer. The corresponding CSC values were 1733 ± 12 µC $cm^{-2}$ for PEDOT@CAZ, 493 ± 18 µC $cm^{-2}$ for PEDOT, and 115 ± 5 µC $cm^{-2}$ for ITO/PET (**Figure 17D**). The much larger response of PEDOT@CAZ shows that the drug-loaded coating remained electrochemically accessible to bacterial metabolites even though its abiotic charge-transfer resistance was high.[35,55]

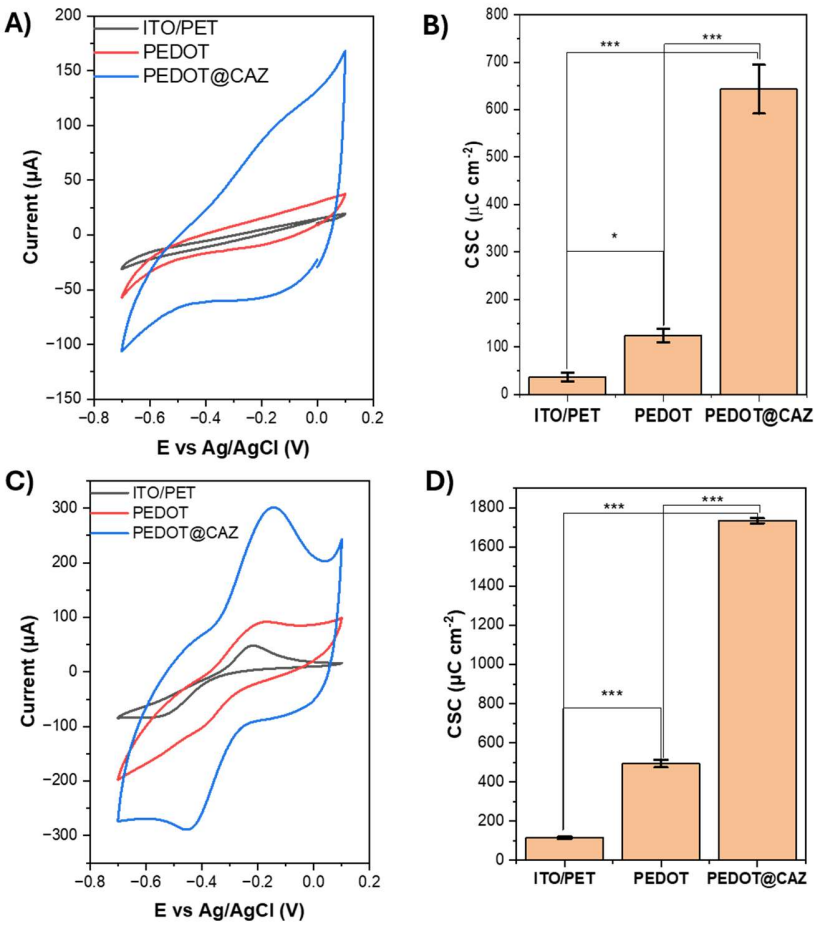



***Figure 17**: Cyclic voltammetry and charge-storage capacity of ITO/PET, PEDOT, and PEDOT@CAZ after exposure to S. oneidensis (A and B) and P. aeruginosa (C and D). Adapted from Figure 5 in [R5]. Copyrights (2026) Advanced Materials Interfaces published by Wiley-VCH GmbH.*

Further EIS studies revealed that in the presence of *S. oneidensis*, the Rct of PEDOT@CAZ decreased to 1220 ± 34 Ω and was lower than the 1795 ± 63 Ω measured for PEDOT (**Figure 18A, B**). This suggests that the biofilm introduced an electron-transfer pathway that partly compensated for the resistive effect of CAZ. The result is consistent with direct contact through outer-membrane cytochromes and mediated transfer by flavins.[20,56]

The response to *P. aeruginosa* was the opposite. PEDOT alone exhibited a low Rct of 117 ± 2 Ω, whereas PEDOT@CAZ reached 11.6 ± 3.2 kΩ (**Figure 18C, D**). One plausible interpretation is that local CAZ release suppressed phenazine production, nanowire development, or the establishment of an electrically connected biofilm at the drug-loaded surface. Surface fouling and polymer passivation may also have contributed to the observed phenomenon. The data therefore do not support a single universal mechanism. Instead, they show that the same coating can be reduced, oxidized, or passivated differently depending on bacterial physiology and the local antibacterial effect.[35,55]

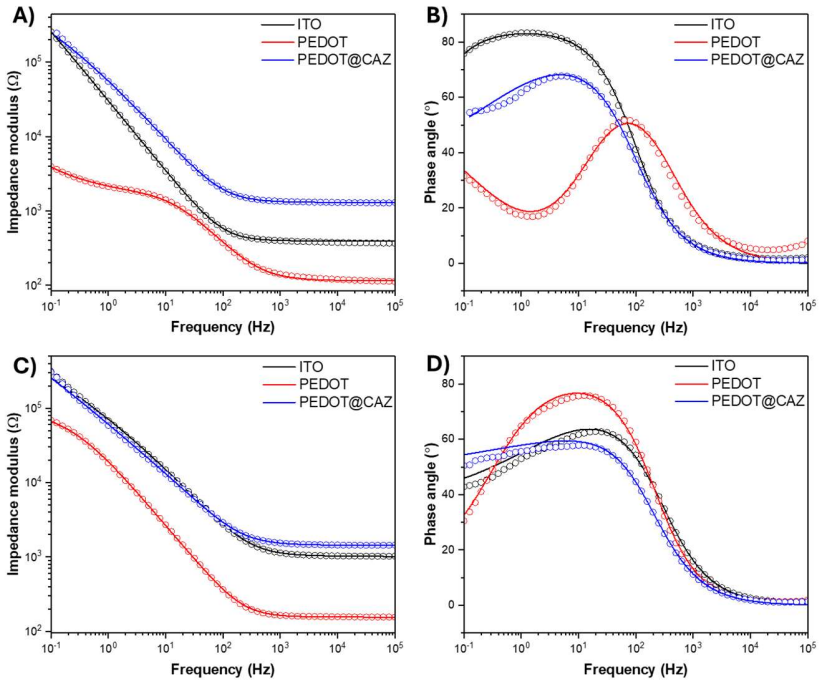



***Figure 18**: Impedance modulus and phase-angle response of ITO/PET, PEDOT, and PEDOT@CAZ in the presence of S. oneidensis (A and B), and P. aeruginosa (C and D). Adapted from Figure 6 in [R5]. Copyrights (2026) Advanced Materials Interfaces published by Wiley-VCH GmbH.*

### *4.5.6. Spectroelectrochemical evidence and short-time redox dynamics*

The optical response of PEDOT was first calibrated by applying potentials from +0.5 V to -0.5 V. More negative potentials increased absorption in the visible region between 400 and 600 nm, while a positive potential enhanced the broad 700-800 nm contribution associated with oxidized charge carriers (**Figure 19A, B**). The calibration confirmed that changes in the polymer doping state could be monitored spectroscopically, providing an independent measure of redox behaviour rather than relying solely on current-based measurements.[21,22]

After 24 h of bacterial exposure, neither organism produced a spectral profile identical to that of the fully oxidized or fully reduced reference state. Instead, *S. oneidensis* and *P. aeruginosa* showed distinct intermediate spectra, indicating partial and spatially heterogeneous redox modification of the polymer film. This is the behaviour expected at a living interface. Electron transfer occurs locally, varies with metabolic state and biofilm thickness, and competes with oxygen, soluble mediators, and ion movement. The spectroscopic result therefore supports the central premise of the coating without implying complete bulk reduction of PEDOT.[35,57]

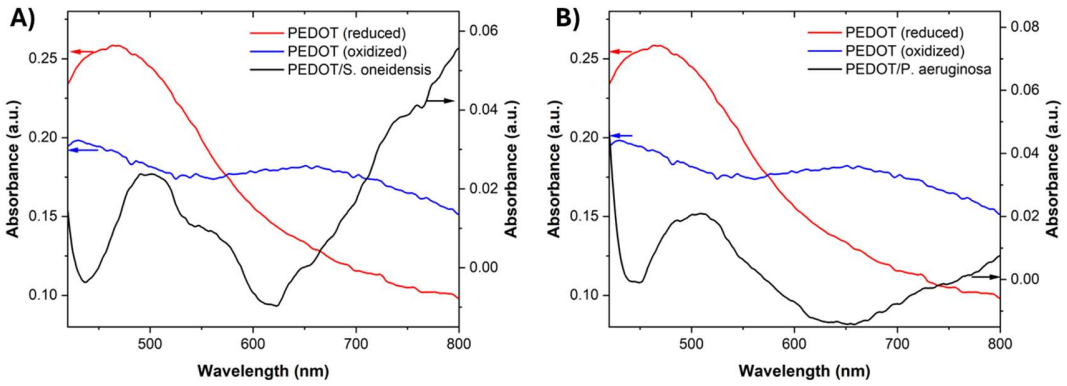



***Figure 19**: UV-Vis spectra showing the redox-dependent optical response of PEDOT after exposure to S. oneidensis (A), and P. aeruginosa (B). Adapted from Figure 7 in [R5]. Copyrights (2026) Advanced Materials Interfaces published by Wiley-VCH GmbH.*

Furthermore, OCP, chronoamperometry, and chronopotentiometry provided a time-domain view of these interactions. With *S. oneidensis*, PEDOT@CAZ began at a higher OCP than PEDOT and showed a larger potential decay over 60 s. At a fixed

potential, its current declined from approximately 1.9 to 0.5 µA, more sharply than the response of pristine PEDOT. Under constant current, PEDOT@CAZ also displayed a more pronounced potential increase. Together, these results indicated that CAZ incorporation altered the kinetics and sensitivity of redox exchange with *S. oneidensis*.[20,56] The corresponding OCP, chronoamperometric, and chronopotentiometric figures are available in the Appendix [**R5**].

On the other hand, *P. aeruginosa* produced a different pattern. The OCP of PEDOT@CAZ was lower than that of PEDOT, while the chronoamperometric current response of the drug-loaded film was much larger. This behaviour is compatible with stronger coupling to soluble redox metabolites but also with rapid modification of the interface as CAZ was released.

### *4.5.7. Antibacterial and antibiofilm performance*

Prior to analysing the antibacterial activity of the coatings, the minimum inhibitory concentration (MIC) of free CAZ was determined for both electroactive species. The MIC was 2.0 ± 1.0 µg $mL^{-1}$ for *S. oneidensis* and 5.0 ± 1.0 µg $mL^{-1}$ for *P. aeruginosa*. The higher value observed for *P. aeruginosa* was consistent with its greater intrinsic resistance and faster growth profile.[9]

The biological response at the material interface was prominent after 24 h. For *S. oneidensis*, the optical density decreased from 0.24 ± 0.01 with ITO/PET to 0.19 ± 0.01 with PEDOT and 0.11 ± 0.01 with PEDOT@CAZ (**Figure 20A**). Biofilm coverage fell from 23.4 ± 1.3% on ITO/PET and 18.2 ± 3.9% on PEDOT to 6.5 ± 1.3% on PEDOT@CAZ (**Figure 20B**). Confocal analysis showed only 13 ± 2.4% of viable cells on the drug-loaded coating, compared with 62 ± 6.8% on PEDOT and 92 ± 2.7% on ITO/PET (**Figure 20C, E**).[48,51]

Against *P. aeruginosa*, the PEDOT@CAZ limited the OD to 0.47 ± 0.01, compared with 0.53 ± 0.01 for PEDOT and 0.65 ± 0.01 for ITO/PET (**Figure 20A**). Biofilm coverage decreased to 16.5 ± 3.3% (**Figure 20B**), while cell viability at the surface was reduced to 20 ± 8.2%. The corresponding values were 34.1 ± 9.9% biofilm and 69 ± 4.1% viability on PEDOT, and 49.4 ± 12.1% biofilm and 95 ± 3.3% viability on ITO/PET (**Figure 20D, F**).[27,48]

Planktonic growth was observed even though the total measured CAZ release exceeded the MIC. The following reasons explain this phenomenon. HPLC measures total CAZ in the collected medium, not necessarily the fraction that remains intact and biologically active. Ceftazidime can hydrolyse during incubation, adsorb to cells or extracellular material, and be degraded by beta-lactamases. More importantly, the coating generated a localized release zone at the polymer-biofilm interface. The strongest effect was therefore expected on adhesion and surface-associated cells rather than throughout the entire planktonic population. This distinction is central to the proposed application, where preventing colonization of the device surface is more important than sterilizing the surrounding fluid.[54,58]

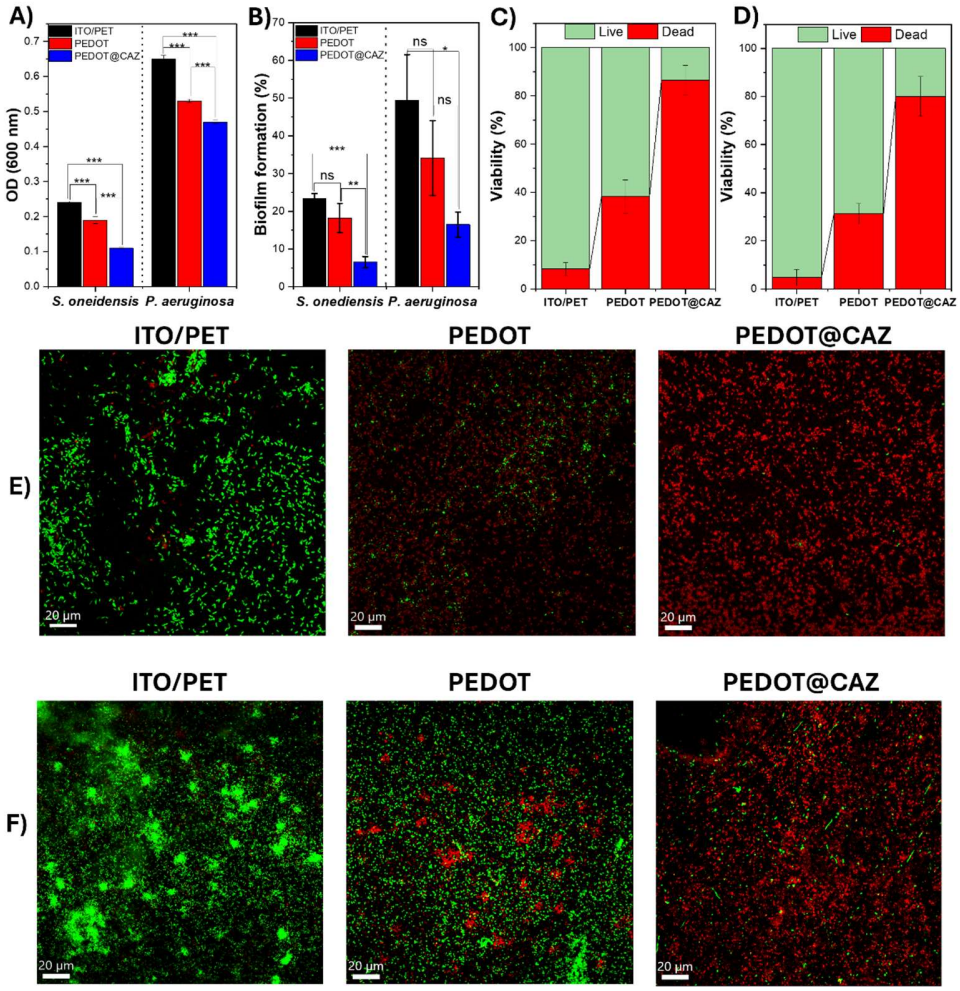



***Figure 20**: Optical density (A), biofilm formation (B), bacterial viability of S. oneidensis (C), and P. aeruginosa (D). Confocal LIVE/DEAD images for S. oneidensis (E), and P. aeruginosa (F) on ITO/PET, PEDOT, and PEDOT@CAZ. Adapted from Figure 10 in [R5]. Copyrights (2026) Advanced Materials Interfaces published by Wiley-VCH GmbH.*

### *4.5.8. Long-term performance, bacterial morphology, and cytocompatibility*

The coating retained its antibacterial activity over eight days of repeated bacterial exposure, although biofilm formation fluctuated over time rather than following a consistent linear trend. For *S. oneidensis*, PEDOT@CAZ limited biofilm formation to 6.5 ± 1.3% on day 1, increased to 16.9 ± 0.3% by day 3, fell to 4.4 ± 2.5% on day 5, and ended at 7.0 ± 1.6% on day 8. The mean over the full period was 12.1 ± 1.7% (**Figure 21A**). *P. aeruginosa* produced higher and more variable colonization, with values of 16.5 ± 3.3%, 14.3 ± 0.1%, 6.1 ± 0.1%, and 29.1 ± 1.1% at the corresponding time points and an overall mean of 17.7 ± 0.9% (**Figure 21B**). [18,59]

The rise-and-fall pattern is biologically plausible. Biofilms pass through attachment, microcolony growth, maturation, restructuring, and dispersal. Nutrient and oxygen gradients, waste accumulation, quorum sensing, and changes in antibiotic availability can all reduce biomass after an earlier increase. The non-linear release profile of PEDOT@CAZ likely added another source of temporal variation. The long-term experiment therefore supported sustained function, but it also showed that a responsive coating interacts with a changing biological system rather than imposing a constant inhibition rate.[7,18]

SEM revealed a pronounced morphological response of *S. oneidensis* on PEDOT@CAZ. Cells increased in length to approximately 3.33 ± 0.97 µm and became narrower, compared with cells on ITO/PET or PEDOT (**Figure 21C**). This elongation may reflect cellular stress, delayed septation, or altered cell-division dynamics in response to β-lactam exposure. *P. aeruginosa* did not exhibit the same degree of cell elongation (**Figure 21D**); however, extracellular matrix material remained visible on all surfaces, consistent with its ability to maintain a structured biofilm even under antimicrobial pressure.[27,58]

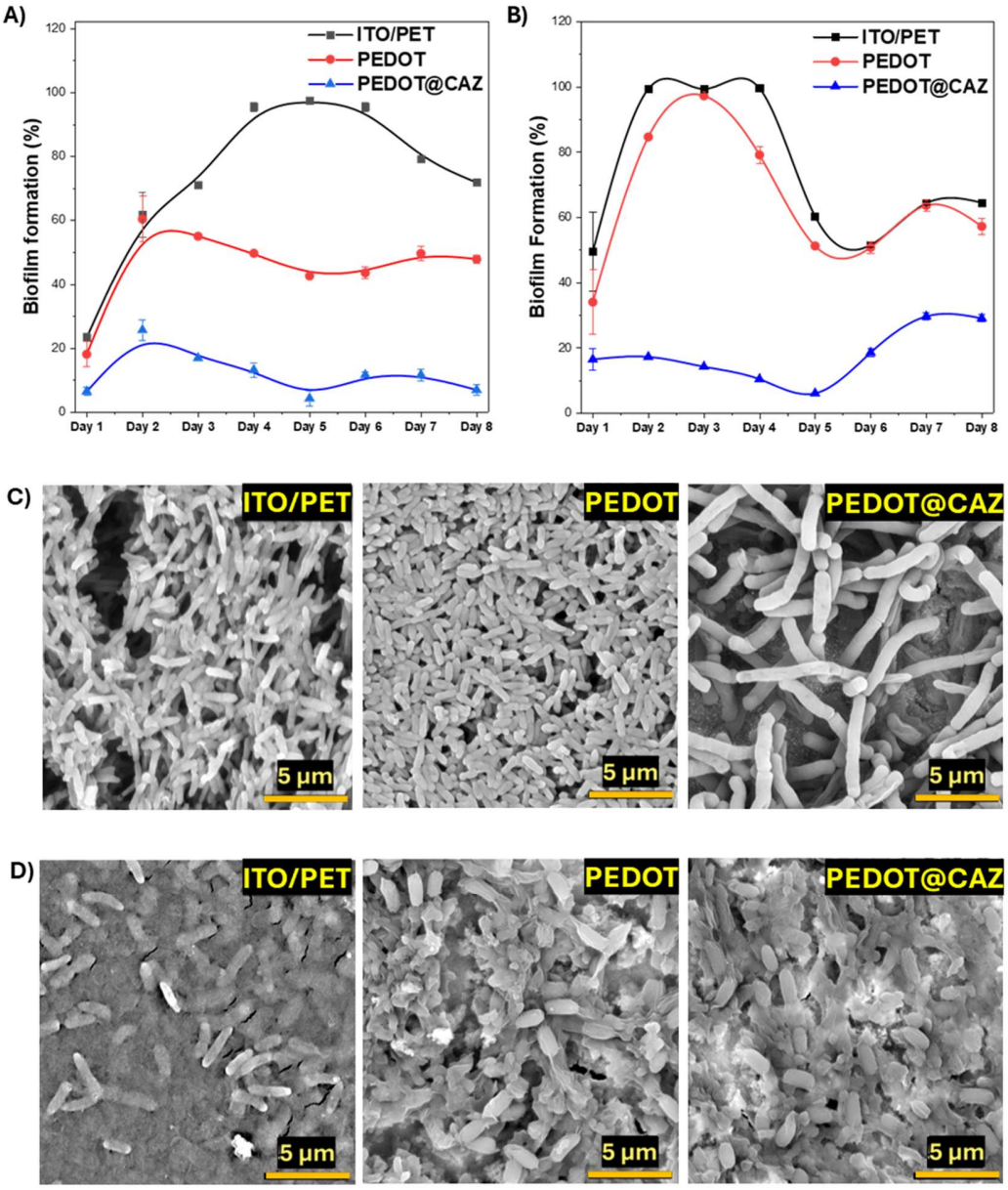



***Figure 21**: Eight-day biofilm response of S. oneidensis (A), and P. aeruginosa (B). SEM morphology of S. oneidensis (C) and P. aeruginosa (D) on ITO/PET, PEDOT, and PEDOT@CAZ. Adapted from Figure 11 in [R5]. Copyrights (2026) Advanced Materials Interfaces published by Wiley-VCH GmbH.*

Cytocompatibility was assessed with normal human dermal fibroblasts. PEDOT supported 85.5 ± 12.5% metabolic activity, while PEDOT@CAZ supported 84.7 ± 7.6%; the ITO/PET value was 78.7 ± 8.1%. All values remained above the 70% threshold commonly used to indicate non-cytotoxicity under the ISO 10993-5 framework. These

findings suggested that incorporation of CAZ did not induce acute cytotoxicity under the tested conditions. Although this assessment did not replace longer-term or in vivo evaluation, it demonstrated that antibacterial functionality was achieved without an immediate loss of mammalian cell compatibility.[29,39]

### *4.5.9. Mechanistic interpretation, novelty, and remaining questions*

The available data supported a working mechanism in which electroactive bacteria alter the local redox state of PEDOT through direct or mediated extracellular electron transfer.[60] This redox switching changed the charge state of the polymer, counter-ion distribution, chain conformation, and wettability. These changes can weaken the interactions responsible for retaining CAZ and facilitate its release from the coating. *P. aeruginosa* induced greater drug release, likely because diffusible phenazines can undergo repeated redox cycling between the biofilm and the polymer. In contrast, *S. oneidensis* produced a somewhat lower response through cytochrome- and flavin-dependent electron-transfer pathways. Once released, CAZ inhibited cell-wall synthesis near the coating surface, thereby reducing bacterial viability and slowing biofilm formation.[35,57]

The novelty of this study lies in linking bacterial activity directly to drug release. Conventional conducting-polymer systems typically release therapeutic agents in response to an externally applied potential. PEDOT@CAZ retains this externally controlled function but is also capable of responding without operator intervention. Passive drug leakage remains low, while the antibacterial response is concentrated at locations where bacteria exchange electrons with the coating. This creates a localized feedback mechanism in which increased bacterial redox activity promotes greater CAZ release, while the released antibiotic, in turn, suppresses the biofilm responsible for generating the redox signal.[24,45]

The current experiments demonstrate an association between bacterial activity and drug release, together with species-dependent behaviour and several converging electrochemical observations. However, they do not fully separate the contribution of extracellular electron transfer from other bacterial processes. A more definitive mechanistic study should therefore compare wild-type strains with EET-deficient mutants, include heat-killed controls, examine purified phenazines and flavins at controlled

concentrations, and quantify drug release under matched biomass and oxygen conditions. Real-time monitoring of drug release would also help establish a clearer link between individual redox events and molecular transport through the polymer. In addition, film thickness, drug loading, and mechanical stability should be optimized to extend the functional lifetime of the coating beyond the current 120-cycle stability limit and to minimize drug depletion during prolonged exposure.[4,56]

Despite these limitations, this study brought together the main ideas developed throughout the thesis. The glucose and calcium studies showed how PEDOT-based interfaces could be tailored to support electroactive bacteria and improve their interaction with the electrode. The DTAB study then demonstrated that an antibacterial compound could be incorporated into PEDOT and released through electrical stimulation. PEDOT@CAZ built on both findings by creating a bacteria-responsive system in which bacterial activity contributed to triggering the release of the antibacterial agent. In this way, the coating did more than simply carry an antibiotic; it responded to biological activity occurring at the interface.

**In this chapter, I developed a PEDOT@CAZ interface that functions as a bacteria-responsive antibacterial coating in which the redox activity of electroactive bacteria is associated with the release of ceftazidime from the PEDOT matrix. Passive drug leakage remained low, whereas electrical stimulation and exposure to *S. oneidensis* and *P. aeruginosa* produced substantially higher CAZ release, with species-dependent electrochemical and spectroscopic responses reflecting their different extracellular electron-transfer pathways. The released CAZ reduced bacterial viability and biofilm formation at the material interface, while the coating retained antibacterial activity during prolonged incubation and remained compatible with human dermal fibroblasts. These findings indicate that PEDOT@CAZ can combine redox responsiveness, localized antibiotic delivery, antibiofilm activity, and cytocompatibility within a single coating. Although further studies are required to separate the contribution of extracellular electron transfer from other bacterial processes and to improve long-term stability, the PEDOT@CAZ system represents the main outcome of this dissertation and provides a basis for the future development of bacteria-responsive coatings for biomedical applications.[3,9]**

# 5. Summary

This dissertation examined conducting-polymer interfaces as dynamic bioelectrochemical systems in which material properties and bacterial behaviour were closely interconnected. The work began with a critical review of electrically conducting biohybrids and then developed through four experimental approaches: organic functionalization of PEDOT:PSS, modification with metal ions, surfactant doping of PEDOT, and incorporation of ceftazidime into a redox-active PEDOT matrix. Together, these studies explored how relatively simple changes in interfacial chemistry can redirect the same class of materials toward either supporting beneficial bacterial activity or suppressing unwanted colonization.

The first part showed that immobilization, cell viability, and extracellular electron transfer are closely interconnected and should not be considered separately. Conducting polymers provide a matrix that supports both electronic and ionic transport, while electroactive microorganisms contribute redox proteins, soluble mediators, and other structures involved in electron transfer. Effective interface design therefore requires attention to both sides of the system: the intrinsic electrochemical properties of the coating and the biological pathways through which bacteria exchange electrons with the material.[3,4]

Organic surface modification showed that glucose transformed PEDOT:PSS from a surface with limited bacterial colonization into a more favourable interface for *S. oneidensis*. Although the glucose layer reduced the abiotic current response and charge-storage capacity, it promoted biofilm formation, maintained high bacterial viability, and improved the overall bacteria–electrode interaction. Metal-ion modification provided a different route toward the same objective. Among the ions investigated, calcium produced the most favourable combination of surface roughness, wettability, bacterial viability, biofilm formation, and charge-storage behaviour, whereas barium shifted the response in the opposite direction by promoting bacterial inhibition.

The PEDOT@DTAB study shifted the focus from promoting biofilm formation to controlling bacterial colonization. DTAB influenced polymer growth, increased charge-storage capacity, and introduced a cationic, membrane-active antibacterial component that could be released either passively or in response to electrical stimulation. The coating

showed a stronger inhibitory effect against *S. oneidensis* than against *P. aeruginosa*, demonstrating that antibacterial performance remained species dependent even when the underlying chemical mechanism of the coating was well defined.

The primary PEDOT@CAZ study brought the findings from the earlier work together. Ceftazidime was incorporated during PEDOT electropolymerization without compromising the film's charge-storage properties. Passive release remained low, whereas electrical cycling and exposure to electroactive bacteria markedly increased CAZ release. In contrast, control conditions involving non-electroactive microorganisms and pH-adjusted media produced little or no detectable release. These findings supported the link between bacterial redox activity and drug transport through the PEDOT matrix.

The antibacterial activity was concentrated at the material–bacteria interface. PEDOT@CAZ reduced bacterial viability and biofilm formation, retained antibacterial activity during prolonged exposure, and remained compatible with normal human dermal fibroblasts. Overall, the coating combined redox responsiveness, localized drug release, antibiofilm activity, and initial mammalian-cell compatibility within a single material platform.

Taken together, the five articles supported a modular approach to the design of conducting-polymer biointerfaces. Glucose and calcium can be used to create conditions that favour the development and electrochemical activity of an electroactive biofilm, whereas DTAB and CAZ are more suitable when bacterial colonization needs to be suppressed. A central design principle emerging from this work is that the redox state of PEDOT should not be viewed merely as an electrochemical parameter. Rather, it represents a controllable link between bacterial metabolism and material function.

The next critical stage is to examine the PEDOT@CAZ system from both mechanistic and translational perspectives. Further mechanistic studies should include EET-deficient bacterial mutants, mediator-only controls, heat-killed cells, and real-time release measurements to define the triggering process more precisely. At the same time, the coating should be optimized in terms of mechanical stability, drug loading, long-term performance, and application to device-relevant geometries. These studies will help determine whether the concept can be translated to catheters, wound dressings, implant

coatings, and other biomedical devices in which early detection and suppression of bacterial colonization are particularly important.

# 6. Literature

(1) Donahue, M. J.; Sanchez-Sanchez, A.; Inal, S.; Qu, J.; Mecerreyes, D.; Malliaras, G. G.; Martin, D. C.; Owens, R. M. Tailoring PEDOT properties for applications in bioelectronics. Materials Science and Engineering: R: Reports 2020, 140, 100546. https://doi.org/10.1016/j.mser.2020.100546.

(2) Tomczykowa, M.; Płońska-Brzezińska, M. E. Conducting polymers, hydrogels and their composites: Preparation, properties and bioapplications. Polymers 2019, 11, 350. https://doi.org/10.3390/polym11020350.

(3) Abdullah; Krukiewicz, K. Development of electrically-conducting biohybrid materials based on electroactive bacteria and conjugated polymers: Review and perspectives. Electrochimica Acta 2023, 468, 143191. https://doi.org/10.1016/j.electacta.2023.143191.

(4) Patil, S. A.; Hägerhäll, C.; Gorton, L. Electron transfer mechanisms between microorganisms and electrodes in bioelectrochemical systems. Bioanalytical Reviews 2012, 4, 159–192. https://doi.org/10.1007/s12566-012-0033-x.

(5) Zheng, S.; Bawazir, M.; Dhall, A.; Kim, H. E.; He, L.; Heo, J.; Hwang, G. Implication of surface properties, bacterial motility, and hydrodynamic conditions on bacterial surface sensing and their initial adhesion. Frontiers in Bioengineering and Biotechnology 2021, 9, 643722. https://doi.org/10.3389/fbioe.2021.643722.

(6) Yoda, I.; Koseki, H.; Tomita, M.; Shida, T.; Horiuchi, H.; Sakoda, H.; Osaki, M. Effect of surface roughness of biomaterials on Staphylococcus epidermidis adhesion. BMC Microbiology 2014, 14, 234. https://doi.org/10.1186/s12866-014-0234-2.

(7) Donlan, R. M. Biofilms: Microbial life on surfaces. Emerging Infectious Diseases 2002, 8, 881–890. https://doi.org/10.3201/eid0809.020063.

(8) Koo, H.; Allan, R. N.; Howlin, R. P.; Stoodley, P.; Hall-Stoodley, L. Targeting microbial biofilms: Current and prospective therapeutic strategies. Nature Reviews Microbiology 2017, 15, 740–755. https://doi.org/10.1038/nrmicro.2017.99.

(9) Abdullah; Smołka, S.; Ayaz, K.; Shakibania, S.; Maryam, S.; Patel, T.; Turczyn, R.; Zabłocka-Godlewska, E.; Krukiewicz, K. Smart antibacterial coatings: Harnessing

bacterial redox activity for infection control. Advanced Materials Interfaces 2026, e70647. https://doi.org/10.1002/admi.70647.

(10) Gomez-Carretero, S.; Libberton, B.; Svennersten, K.; Persson, K.; Jager, E.; Berggren, M.; Rhen, M.; Richter-Dahlfors, A. Redox-active conducting polymers modulate Salmonella biofilm formation by controlling availability of electron acceptors. npj Biofilms and Microbiomes 2017, 3, 19. https://doi.org/10.1038/s41522-017-0027-0.

(11) Masi, E.; Ciszak, M.; Santopolo, L.; Frascella, A.; Giovannetti, L.; Marchi, E.; Viti, C.; Mancuso, S. Electrical spiking in bacterial biofilms. Journal of the Royal Society Interface 2015, 12, 20141036. https://doi.org/10.1098/rsif.2014.1036.

(12) Abdullah; Shakibania, S.; Patel, T.; Shyntum, D. Y.; Krukiewicz, K. Surface-functionalized PEDOT:PSS interfaces for improved adhesion, viability, and extracellular charge transfer of Shewanella oneidensis MR-1. ACS Sustainable Chemistry & Engineering 2024, 12, 18508–18521. https://doi.org/10.1021/acssuschemeng.4c05458.

(13) Abdullah; Shyntum, D. Y.; Shakibania, S.; Patel, T.; Krukiewicz, K. Engineering conducting polymer-based interfaces for high-performance microbial electrochemical systems. Bioelectrochemistry 2026, 168, 109142. https://doi.org/10.1016/j.bioelechem.2025.109142.

(14) Abdullah; Shakibania, S.; Zabłocka-Godlewska, E.; Aniołek, K.; Krukiewicz, K. Surfactant-doped PEDOT films as dual-function bioelectronic coatings with enhanced charge storage capacity and antibiofilm activity. Bioelectrochemistry 2026, 172, 109366. https://doi.org/10.1016/j.bioelechem.2026.109366.

(15) Yong, Y.-C.; Cai, Z.; Yu, Y.-Y.; Chen, P.; Jiang, R.; Cao, B.; Sun, J.-Z.; Wang, J.-Y.; Song, H. Increase of riboflavin biosynthesis underlies enhancement of extracellular electron transfer of Shewanella in alkaline microbial fuel cells. Bioresource Technology 2013, 130, 763–768. https://doi.org/10.1016/j.biortech.2012.11.145.

(16) Krukiewicz, K.; Stokfisz, A.; Zak, J. K. Two approaches to the model drug immobilization into conjugated polymer matrix. Materials Science and Engineering: C 2015, 54, 176–181. https://doi.org/10.1016/j.msec.2015.05.017.

(17) Donlan, R. M.; Costerton, J. W. Biofilms: Survival mechanisms of clinically relevant microorganisms. Clinical Microbiology Reviews 2002, 15, 167–193. https://doi.org/10.1128/CMR.15.2.167-193.2002.

(18) Sauer, K.; Stoodley, P.; Goeres, D. M.; Hall-Stoodley, L.; Burmølle, M.; Stewart, P. S.; Bjarnsholt, T. The biofilm life cycle: Expanding the conceptual model of biofilm formation. Nature Reviews Microbiology 2022, 20, 608–620. https://doi.org/10.1038/s41579-022-00767-0.

(19) Nguyen, A. S.; Musiani, M.; Orazem, M. E.; Pébère, N.; Tribollet, B.; Vivier, V. Impedance analysis of the distributed resistivity of coatings in dry and wet conditions. Electrochimica Acta 2015, 179, 452–459. https://doi.org/10.1016/j.electacta.2015.02.109.

(20) Baron, D.; LaBelle, E.; Coursolle, D.; Gralnick, J. A.; Bond, D. R. Electrochemical measurement of electron transfer kinetics by Shewanella oneidensis MR-1. Journal of Biological Chemistry 2009, 284, 28865–28873. https://doi.org/10.1074/jbc.M109.043455.

(21) Rybakiewicz-Sekita, R.; Gryszel, M.; Pathak, G.; Gańczarczyk, R.; Donahue, M. J.; Głowacki, E. D. Well-defined electrochemical switching of amphiphilic glycolated poly(3,4-ethylenedioxythiophene). Journal of Materials Chemistry C 2022, 10, 17208–17215. https://doi.org/10.1039/d2tc01448c.

(22) Chen, X.; Zhang, J. Blue-to-transmissive electrochromic poly(2,3-dimethyl-2,3-dihydrothieno[3,4-b][1,4]dioxine) (PEDOT-Me2) with improved optical contrast. Journal of Solid State Electrochemistry 2020, 24, 441–445. https://doi.org/10.1007/s10008-019-04343-0.

(23) Safdari, M.; Shakiba, E.; Kiaie, S. H.; Fattahi, A. Preparation and characterization of ceftazidime-loaded electrospun silk fibroin/gelatin mat for wound dressing. Fibers and Polymers 2016, 17, 744–750. https://doi.org/10.1007/s12221-016-5822-3.

(24) Pérez-Nava, A.; González-Campos, J. B.; Frontana-Uribe, B. A. Conducting polymers for in situ drug release triggered via electrical stimulus. ACS Applied Polymer Materials 2024, 6, 9375–9395. https://doi.org/10.1021/acsapm.4c01013.

(25) Myers, C. M.; Blumer, J. L. Determination of ceftazidime in biological fluids by using high-pressure liquid chromatography. Antimicrobial Agents and Chemotherapy 1983, 24, 343–346. https://doi.org/10.1128/AAC.24.3.343.

(26) Hsueh, S. C.; Lee, Y. J.; Huang, Y. T.; Liao, C. H.; Tsuji, M.; Hsueh, P. R. In vitro activities of cefiderocol, ceftolozane/tazobactam, ceftazidime/avibactam and other comparative drugs against imipenem-resistant Pseudomonas aeruginosa and Acinetobacter baumannii, and Stenotrophomonas maltophilia, all associated with bloodstream infections in Taiwan. Journal of Antimicrobial Chemotherapy 2019, 74, 380–386. https://doi.org/10.1093/jac/dky425.

(27) Richards, D. M.; Brogden, R. N. Ceftazidime. A review of its antibacterial activity, pharmacokinetic properties and therapeutic use. Drugs 1985, 29, 105–161. https://doi.org/10.2165/00003495-198529020-00002.

(28) Leuko, S.; Legat, A.; Fendrihan, S.; Stan-Lotter, H. Evaluation of the LIVE/DEAD BacLight kit for detection of extremophilic archaea and visualization of microorganisms in environmental hypersaline samples. Applied and Environmental Microbiology 2004, 70, 6884–6886. https://doi.org/10.1128/AEM.70.11.6884-6886.2004.

(29) International Organization for Standardization. ISO 10993-5:2009, Biological evaluation of medical devices—Part 5: Tests for in vitro cytotoxicity; ISO: Geneva, Switzerland, 2009. https://www.iso.org/standard/36406.html

(30) Gião, M. S.; Montenegro, M. I.; Vieira, M. J. Monitoring biofilm formation by using cyclic voltammetry-Effect of the experimental conditions on biofilm removal and activity. Water Science and Technology 2003, 47, 51–56. https://doi.org/10.2166/wst.2003.0278.

(31) Ateh, D. D.; Navsaria, H. A.; Vadgama, P. Polypyrrole-based conducting polymers and interactions with biological tissues. Journal of the Royal Society Interface 2006, 3, 741–752. https://doi.org/10.1098/rsif.2006.0141.

(32) Song, R.-B.; Wu, Y.-C.; Lin, Z.-Q.; Xie, J.; Tan, C. H.; Loo, J. S. C.; Cao, B.; Zhang, J.-R.; Zhu, J.-J.; Zhang, Q. Living and conducting: Coating individual bacterial cells with in situ formed polypyrrole. Angewandte Chemie International Edition 2017, 56, 10516–10520. https://doi.org/10.1002/anie.201704729.

(33) Zeglio, E.; Rutz, A. L.; Winkler, T. E.; Malliaras, G. G.; Herland, A. Conjugated polymers for assessing and controlling biological functions. Advanced Materials 2019, 31, e1806712. https://doi.org/10.1002/adma.201806712.

(34) Marsili, E.; Baron, D. B.; Shikhare, I. D.; Coursolle, D.; Gralnick, J. A.; Bond, D. R. Shewanella secretes flavins that mediate extracellular electron transfer. Proceedings of the National Academy of Sciences 2008, 105, 3968–3973. https://doi.org/10.1073/pnas.0710525105.

(35) Franco, A.; Chukwubuikem, A.; Meiners, C.; Rosenbaum, M. A. Exploring phenazine electron transfer interaction with elements of the respiratory pathways of Pseudomonas putida and Pseudomonas aeruginosa. Bioelectrochemistry 2024, 157, 108636. https://doi.org/10.1016/j.bioelechem.2023.108636.

(36) Zajdel, T. J.; Baruch, M.; Méhes, G.; Stavrinidou, E.; Berggren, M.; Maharbiz, M. M.; Simon, D. T.; Ajo-Franklin, C. M. PEDOT:PSS-based multilayer bacterial-composite films for bioelectronics. Scientific Reports 2018, 8, 15293. https://doi.org/10.1038/s41598-018-33521-9.

(37) Baker, I. R.; Conley, B. E.; Gralnick, J. A.; Girguis, P. R. Evidence for horizontal and vertical transmission of Mtr-mediated extracellular electron transfer among the bacteria. mBio 2022, 13, e02904-21. https://doi.org/10.1128/MBIO.02904-21.

(38) Zhao, Q.; Jamal, R.; Zhang, L.; Wang, M.; Abdiryim, T. The structure and properties of PEDOT synthesized by template-free solution method. Nanoscale Research Letters 2014, 9, 557. https://doi.org/10.1186/1556-276X-9-557.

(39) Gupta, S.; Datt, R.; Mishra, A.; Tsoi, W. C.; Patra, A.; Bober, P. Poly(3,4-ethylenedioxythiophene):poly(styrene sulfonate) in antibacterial, tissue engineering and biosensors applications: Progress, challenges and perspectives. Journal of Applied Polymer Science 2022, 139, e52663. https://doi.org/10.1002/app.52663.

(40) Cloutier, M.; Mantovani, D.; Rosei, F. Antibacterial coatings: Challenges, perspectives, and opportunities. Trends in Biotechnology 2015, 33, 637–652. https://doi.org/10.1016/j.tibtech.2015.09.002.

(41) Li, C.; Hu, S.; Ji, C.; Yi, K.; Yang, W. Insight into the pseudocapacitive behavior of electroactive biofilms in response to dynamic-controlled electron transfer and metabolism kinetics for current generation in water treatment. Environmental Science & Technology 2023, 57, 19891–19901. https://doi.org/10.1021/acs.est.3c04771.

(42) Langer, R.; Peppas, N. Chemical and physical structure of polymers as carriers for controlled release of bioactive agents: A review. Journal of Macromolecular Science, Part C 1983, 23, 61–126. https://doi.org/10.1080/07366578308079439.

(43) Higuchi, T. Mechanism of sustained-action medication. Theoretical analysis of rate of release of solid drugs dispersed in solid matrices. Journal of Pharmaceutical Sciences 1963, 52, 1145–1149. https://doi.org/10.1002/jps.2600521210.

(44) Korsmeyer, R. W.; Gurny, R.; Doelker, E.; Buri, P.; Peppas, N. A. Mechanisms of solute release from porous hydrophilic polymers. International Journal of Pharmaceutics 1983, 15, 25–35. https://doi.org/10.1016/0378-5173(83)90064-9.

(45) Boehler, C.; Oberueber, F.; Asplund, M. Tuning drug delivery from conducting polymer films for accurately controlled release of charged molecules. Journal of Controlled Release 2019, 304, 173–180. https://doi.org/10.1016/j.jconrel.2019.05.017.

(46) Gottenbos, B.; Grijpma, D. W.; van der Mei, H. C.; Feijen, J.; Busscher, H. J. Antimicrobial effects of positively charged surfaces on adhering Gram-positive and Gram-negative bacteria. Journal of Antimicrobial Chemotherapy 2001, 48, 7–13. https://doi.org/10.1093/jac/48.1.7.

(47) Akbari Hasanjani, H. R.; Zarei, K. Electrochemical sensor for ultrasensitive determination of ceftazidime using hollow platinum nanoparticles/reduced graphene oxide/pencil graphite electrode. Chemical Papers 2018, 72, 1935–1944. https://doi.org/10.1007/s11696-018-0428-4.

(48) Czerwińska-Główka, D.; Przystaś, W.; Zabłocka-Godlewska, E.; Student, S.; Cwalina, B.; Łapkowski, M.; Krukiewicz, K. Electrically-responsive antimicrobial coatings based on a tetracycline-loaded PEDOT matrix. Materials Science and Engineering: C 2021, 123, 112017. https://doi.org/10.1016/j.msec.2021.112017.

(49) Devi, R.; Thakur, M.; Pundir, C. S. Construction and application of an amperometric xanthine biosensor based on zinc oxide nanoparticles-polypyrrole composite film. Biosensors and Bioelectronics 2011, 26, 3420–3426. https://doi.org/10.1016/j.bios.2011.01.014.

(50) De Haro Moreno, A.; Regina Nunes Salgado, H. Development and validation of the quantitative analysis of ceftazidime in powder for injection by infrared spectroscopy. Physical Chemistry 2012, 2, 6–11. https://doi.org/10.5923/j.pc.20120201.02.

(51) Enshaei, H.; Puiggalí-Jou, A.; del Valle, L. J.; Turon, P.; Saperas, N.; Alemán, C. Nanotheranostic interface based on antibiotic-loaded conducting polymer nanoparticles for real-time monitoring of bacterial growth inhibition. Advanced Healthcare Materials 2021, 10, 2001636. https://doi.org/10.1002/adhm.202001636.

(52) Krukiewicz, K.; Cichy, M.; Ruszkowski, P.; Turczyn, R.; Jarosz, T.; Zak, J. K.; Łapkowski, M.; Bednarczyk-Cwynar, B. Betulin-loaded PEDOT films for regional chemotherapy. Materials Science and Engineering: C 2017, 73, 611–615. https://doi.org/10.1016/j.msec.2016.12.115.

(53) Resina, L.; El Hauadi, K.; Sans, J.; Esteves, T.; Ferreira, F. C.; Pérez-Madrigal, M. M.; Alemán, C. Electroresponsive and pH-sensitive hydrogel as carrier for controlled chloramphenicol release. Biomacromolecules 2023, 24, 1432–1444. https://doi.org/10.1021/acs.biomac.2c01442.

(54) Zając, M.; Siwek, J.; Muszalska, I. The mechanism of ceftazidime degradation in aqueous solutions. Acta Poloniae Pharmaceutica—Drug Research 1998, 55, 275–278. https://www.ptfarm.pl/pub/File/Acta_Poloniae/1998/4/275.pdf

(55) Maruthupandy, M.; Anand, M.; Maduraiveeran, G.; Beevi, A. S. H.; Priya, R. J. Electrical conductivity measurements of bacterial nanowires from Pseudomonas aeruginosa. Advances in Natural Sciences: Nanoscience and Nanotechnology 2015, 6, 045007. https://doi.org/10.1088/2043-6262/6/4/045007.

(56) Carmona-Martinez, A. A.; Harnisch, F.; Fitzgerald, L. A.; Biffinger, J. C.; Ringeisen, B. R.; Schröder, U. Cyclic voltammetric analysis of the electron transfer of Shewanella oneidensis MR-1 and nanofilament and cytochrome knock-out mutants. Bioelectrochemistry 2011, 81, 74–80. https://doi.org/10.1016/j.bioelechem.2011.02.006.

(57) Zang, Y.; Cao, B.; Zhao, H.; Xie, B.; Ge, Y.; Liu, H.; Yi, Y. Mechanism and applications of bidirectional extracellular electron transfer of Shewanella. Environmental Science: Processes & Impacts 2023, 25, 1863–1877. https://doi.org/10.1039/d3em00224a.

(58) Boys, M. T. H.; Pletzer, D. A review of recently discovered mechanisms of cephalosporin resistance in Pseudomonas aeruginosa. International Journal of Antimicrobial Agents 2025, 66, 107527. https://doi.org/10.1016/j.ijantimicag.2025.107527.

(59) Thi, M. T. T.; Wibowo, D.; Rehm, B. H. A. Pseudomonas aeruginosa biofilms. International Journal of Molecular Sciences 2020, 21, 8671. https://doi.org/10.3390/ijms21228671.

(60) Zhang, S.; Wang, L.; Wu, L.; Li, Z.; Yang, B.; Hou, Y.; He, Q. Deciphering single-bacterium adhesion behavior modulated by extracellular electron transfer. Nano Letters 2021, 21, 5105–5115. https://doi.org/10.1021/acs.nanolett.1c01062.

## Summary of personal contribution

**[R1] Contribution:** Conceived and structured the scope of the review together with the overall scientific framework concerning electrically conducting biohybrid materials based on electroactive bacteria and conjugated polymers. Conducted the literature survey and critically analysed published studies dealing with bacterial immobilization on conducting polymers, bacterial adhesion, extracellular electron-transfer mechanisms, electroactive microorganisms, and the electrochemical performance of bacteria–polymer biohybrids. Particular attention was given to PEDOT, PEDOT:PSS and polypyrrole, including adsorption, antibody-mediated and electrically induced immobilization strategies, as well as the role of outer-membrane cytochromes, pili, flavins and other redox mediators in extracellular electron transfer. Integrated the available literature into a common framework linking bacterial physiology, polymer properties, immobilization strategy and electrochemical performance. Prepared the original manuscript and organized the literature, figures and discussion of the future perspectives and research gaps in electrically conducting bacterial biohybrids. My formally declared contribution to this publication was Conceptualization and Writing – original draft.

***My overall contribution to this research was equal to 70%***

**[R2] Contribution:** Contributed to the methodology and carried out the experimental investigation of surface-functionalized PEDOT:PSS interfaces intended to improve the adhesion, viability and extracellular electron transfer of *Shewanella oneidensis* MR-1. The experimental work included the preparation and evaluation of PEDOT:PSS coatings modified with glucose, sucrose, maltose, cellulose, chitosan, poly(vinyl alcohol), poly-L-lysine and laminin. Contributed to the physicochemical, biological and electrochemical characterization of these interfaces, including assessment of surface morphology, roughness, wettability, biofilm formation, bacterial viability and electrochemical behaviour. Particular attention was given to the glucose-functionalized PEDOT:PSS interface, which provided the most favourable combination of bacterial adhesion, viability and bacteria–electrode charge transfer. Prepared and organized the experimental results for presentation, produced the data visualizations and figures, and wrote the original draft of the manuscript, including the description and interpretation of the experimental findings. My formally declared contribution to this publication was Methodology, Investigation, Visualization and Writing – original draft.

***My overall contribution to this research was equal to 70%***

**[R3] Contribution:** Conducted the experimental investigation of PEDOT:PSS interfaces modified with biologically relevant metal ions, including $Fe^{3+}$, $Mg^{2+}$, $Mn^{2+}$, $Ca^{2+}$ and $Ba^{2+}$, with the aim of determining how ionic modification influences polymer surface properties, bacterial attachment and electrochemical performance. Contributed to the characterization of the resulting coatings in terms of morphology, elemental composition, surface roughness, wettability, biofilm formation, bacterial viability, charge-storage capacity and interfacial charge-transfer resistance. The study identified calcium modification as the most favourable approach for supporting *S. oneidensis* biofilm formation and electrochemical activity, while barium produced an opposite, more antibacterial response. Prepared the visualization of the experimental results, including figures and graphical presentation of the biological and electrochemical data, and wrote the original draft of the manuscript describing the experimental findings and their significance for microbial electrochemical interfaces. My formally declared contribution to this publication was Investigation, Visualization and Writing – original draft.

***My overall contribution to this research was equal to 70%***

**[R4] Contribution:** Participated in the conceptualization of the study and development of the experimental methodology for preparing surfactant-doped PEDOT coatings with combined electrochemical and antibacterial properties. Conducted the experimental investigation of PEDOT electropolymerized in the presence of dodecyltrimethylammonium bromide (DTAB), including preparation of PEDOT@DTAB coatings and evaluation of their electrochemical, physicochemical and antibacterial properties. Contributed to the investigation of charge-storage capacity, impedance behaviour, surface properties, passive and electrically stimulated DTAB release, biofilm formation and bacterial viability against *S. oneidensis* and *P. aeruginosa*, as well as long-term antibacterial performance. Performed formal analysis of the experimental data and evaluated the relationship between DTAB incorporation, polymer redox behaviour, drug release and antibacterial activity. Prepared the data visualization and figures and wrote the original draft of the manuscript, including the presentation and interpretation of the principal results. My formally declared contribution to this publication was Conceptualization, Methodology, Investigation, Formal analysis, Visualization and Writing – original draft.

***My overall contribution to this research was equal to 70%***

**[R5] Contribution:** Conducted the principal experimental investigation of the bacteria-responsive PEDOT@CAZ coating, which represents the main experimental part of the dissertation. Contributed to the methodology for incorporating ceftazidime into PEDOT during electropolymerization and investigated the resulting coating using electrochemical, physicochemical, microbiological and drug-release methods. The experimental work included characterization of PEDOT@CAZ by cyclic voltammetry, electrochemical impedance spectroscopy, FTIR, EDS, SEM, surface roughness and wettability measurements; determination of passive, electrically stimulated and bacteria-triggered ceftazidime release by HPLC; and investigation of the interaction of the coating with *S. oneidensis* and *P. aeruginosa* using electrochemical and spectroelectrochemical techniques. Contributed to antibacterial and antibiofilm testing, bacterial viability analysis, long-term performance studies and cytocompatibility evaluation. The study demonstrated low passive CAZ leakage but substantially greater release following electrical stimulation and exposure to electroactive bacteria, together with species-dependent electrochemical responses and pronounced antibacterial activity at the material interface. Prepared the visualization of the experimental results and wrote the original draft of the manuscript, including the presentation and interpretation of the main findings. My formally declared contribution to this publication was Investigation, Methodology, Visualization and Writing – original draft.

***My overall contribution to this research was equal to 50%***

# List of Scientific Accomplishments

## *1. Publications and chapters other than those included in the doctoral thesis*

1. Smołka, S.; Tomasiak, A.; Shakibania, S.; **Abdullah**; Ayaz, K.; Patel, T.; Cao, E.; Siwy, Z.; Skonieczna, M.; Zabłocka-Godlewska, E.; Turczyn, R.; Krukiewicz, K. Winning the 'race for the surface': curcumin-loaded PEDOT coatings with enhanced biocompatibility and antibacterial capabilities. *Journal of Materials Chemistry B* 2026. DOI: 10.1039/D6TB01040G.
2. Ayaz, K.; Zabłocka-Godlewska, E.; **Abdullah**; et al. Enhancing microbial adhesion and electron transfer of Shewanella oneidensis MR-1 with polyaniline-glucose-gelatin coating for bioelectrochemical applications. Journal of Environmental Chemical Engineering 2026, 14, 121546. DOI: 10.1016/j.jece.2026.121546.
3. Patel, T.; Shyntum, D. Y.; **Abdullah**; et al. Unlocking the potential of quinoline diazonium salts: An electrochemical approach for engineering antimicrobial surfaces. Surfaces and Interfaces 2026, 95, 109635. DOI: 10.1016/j.surfin.2026.109635.
4. Jakubska, J.; Wawoczny, A.; Kluska, D.; Grzybek, P.; Hudecki, A.; Kołodziej, M.; Jasiak-Jaroń, K.; **Abdullah**; Shyntum, D. Y.; Gołombek, K.; Pakieła, W.; Krukiewicz, K.; Gillner, D.; Dudek, G. Dual functionality of deep eutectic solvents in chitosan-based biodegradable films for food packaging applications. Industrial Crops and Products 2025, 232, 121268. DOI: 10.1016/j.indcrop.2025.121268.
5. Maryam, S.; Ul Haq, I.; Wilk, K.; **Abdullah**; Shakibania, S.; Shyntum, D. Y.; Student, S.; Szewczenko, J.; Krukiewicz, K. Antimicrobial efficacy of ultrasonically deposited poly(vinyl alcohol)/poly(L-lysine)-based coatings for urinary catheters. Surface and Coatings Technology 2025, 133094. DOI: 10.1016/j.surfcoat.2025.133094.
6. Skorupa, M.; Skonieczna, M.; Shyntum, D. Y.; **Abdullah**; Turczyn, R.; Asplund, M.; Krukiewicz, K. Electrografted mixed organic monolayers as antibacterial coatings for implantable biomedical devices. Electrochimica Acta 2024, 492, 144354. DOI: 10.1016/j.electacta.2024.144354.

7. Janik, W.; Nowotarski, M.; Ledniowska, K.; Biernat, N.; **Abdullah**; Shyntum, D. Y.; Krukiewicz, K.; Turczyn, R.; Gołombek, K.; Dudek, G. Effect of time on the properties of bio-nanocomposite films based on chitosan with bio-based plasticizer reinforced with nanofiber cellulose. International Journal of Molecular Sciences 2023, 24(17), 13205. DOI: 10.3390/ijms241713205.

### *2. Scientific conferences and scientific meetings*

1. European Materials Research Society (E-MRS) 2026 Fall Meeting, Warsaw University of Technology, Poland, 14–17 September 2026. ***Contributed as Oral Presentation***
2. 2nd International Online Conference on Functional Biomaterials (IOCFB 2026), 8-10 July 2026. ***Contributed as Oral Presentation***
3. Computational Oncology and Personalized Medicine (COPM 2026), April 29, 2026. ***Contributed as Oral Presentation***
4. Gliwice Scientific Meetings, Silesian University of Technology, Gliwice, Poland, 21–22 November 2025. ***Contributed as Poster Presentation***
5. Polymers 2024 – Polymers for a Safe and Sustainable Future, Athens, Greece, 28–31 May 2024. ***Contributed as Poster Presentation***
6. PartNETships: A Network of Key Collaborations to Bring Research Excellence to the Silesian University of Technology, 16–18 June 2024. ***Contributed as Oral Presentation***
7. International Workshop on "Biophotoelectrochemical Systems: Solar Energy Conversion and Fundamental Investigations", St John's College, Cambridge, United Kingdom, 29–31 March 2023. ***Contributed as Poster Presentation***
8. 37th RoMedINF Conference – "Healthcare Green Digital Ecosystems: From Data Analysis to Digital Twin", West University of Timișoara, Romania, 14–15 September 2023. ***Contributed as Oral Presentation***
9. European Materials Research Society (E-MRS) 2023 Fall Meeting, Warsaw University of Technology, Poland, 18–21 September 2023. ***Contributed as Poster Presentation***

### *3. Participation in research projects*

1. National Science Centre (NCN), Poland – PRELUDIUM BIS [Preludium Bis-2021/43/O/ST5/02623] project "Conducting polymer coatings exhibiting bacteria-responsive antibacterial properties– synthesis, structure, and mutual interactions." Silesian University of Technology, Poland, 2023–2026. ***Role: Main investigator/scientific researcher.***

### *4. Research internships*

1. Department of Neurosciences, Karolinska Institute, Sweden, 15 April–15 June 2025.
2. University of Southern Denmark (SDU), 01-30 August 2023, Denmark

### *5. Other scholarships, fellowships, grants and scientific distinctions*

1. NAWA Academic Exchange Scholarship / National Science Centre, Poland, 2025.
2. Silesian University of Technology Rector Award for Best Publications, 2025.
3. Silesian University of Technology Rector Grant for Publications in Scopus Top 10 Journals, received in 2023, 2024, 2025 and 2026.
4. National Agency for the Academic Exchange (NAWA) / Silesian University of Technology PartNETships Fellowship, 2023.
5. Silesian University of Technology Best Ph.D. Student Award, 2022.
6. Best Oral Presentation Award, at PartNETships: A Network of Key Collaborations to Bring Research Excellence to the Silesian University of Technology, 16–18 June 2024.

### *6. Patent*

1. Hybrid pro-adhesive coating, method of preparation and application, Granted Polish Patent PL.250082, Inventors: Abdullah and Katarzyna Krukiewicz.

# Appendix: Supplementary information

This section contains the published papers included in the doctoral thesis [R1–R5], together with the supplementary information associated with these publications. It also includes the declarations of author contributions and the copyright permissions for figures reproduced or adapted in the thesis.